Dissertation submitted to the
Faculty of Science of the University of Neuchâtel
to obtain the degree of Doctor of Science

Development of microfluidic devices for chemical analysis and fluid handling

by

Giovanni Egidi

Institute of Microtechnology
University of Neuchâtel
Rue Jaquet-Droz 1
CH-2007 Neuchâtel
Switzerland

2004

“Folly is the only thing that keeps youth at a stay
and old age afar off”

THE PRAISE OF FOLLY

Erasmus of Rotterdam

IMPRIMATUR POUR LA THESE

Development of microfluidic devices for chemical analysis and fluid handling

M. Giovanni EGIDI

UNIVERSITE DE NEUCHATEL

FACULTE DES SCIENCES

La Faculté des sciences de l'Université de Neuchâtel, sur le rapport des membres du jury

Mme M. Koudelka-Hep,
MM. N. de Rooij (directeur de thèse)
et J.-C. Fiaccabrino (Marin)

autorise l'impression de la présente thèse.

Neuchâtel, le 7 avril 2004

La doyenne:

Martine Rahier

Abstract

Miniaturization of chemical analysis and synthesis systems improve throughput, performance and accessibility, and lead to significantly reduced costs. In this work are described several components that find place in the process of miniaturization.

This work is developed in the frame of the project CREAM (Cartridges with molecularly imprinted Recognition Elements for Antibiotic residues Monitoring in Milk).

Antibiotics are widely used to treat cows' diseases, and traces can be found in milk some days after treatment. The presence of antibiotics in milk represents a potential human health hazard, and can present problems for cheese and yoghourt makers.

The aim of this work is to produce a device able to detect the presence of antibiotics in milk. This device should be the most compact as possible, and have to reduce the cost of the analysis.

A plastic replication technique by cast molding is developed in order to quickly produce plastic prototypes starting from a master made in silicon and photoresist (SU-8).

By exploiting capillary effect, is developed a stop flow valve. The valve is integrated in a microfluidic device realized by DRIE (Deep Reactive Ion Etching) on a silicon wafer. It consists in a vertical capillary connecting the channel on top of the wafer, to the expansion chamber etched on the back-side. The device is finally closed by anodic bonding with two pyrex lid.

Passive stop flow valves are used to realize a sample metering system. Such a system consists in an introduction port for the sample, a capillary and two valves, one of which acts as air vent.

Furthermore a micro drier is developed using the functioning principle of the stop flow valve. The application of this device it to change the liquid phase of a solution, in particular in the project CREAM in necessary to change an aqueous solution into an almost pure solution of acetonitrile.

A new optical detection cell design is fabricated. It consists on an array of channels open at the end, the meniscus formed at the outlet of each channel provides a direct air-liquid interface to the sample volume, through which light could be injected. This optical detection cell is integrated in a cartridge with a microreactor and a sample metering system. The microreactor is packed with MIPs (Molecular Imprinted Polymers) and characterized from the fluidic point of view. The whole cartridge is finally optically characterized with pyrene butyric acid.

TABLE OF CONTENTS

1 Introduction

1.1 Microfluidics

Research in biotechnology demands a large numbers of experiments, such as analyses of DNA or drugs, screening of patients and combinatorial syntheses. All of these procedures require the handling of fluids. As the number of experiments is growing each day, the devices used to carry out the experiments have shrunk, and the strategy of "smaller is better" has begun to transform the world of fluidics as it has revolutionized the world of electronics with the invention of the transistor. A large number of biotechnological applications need to manipulate fluids moving in small channels, a field called microfluidics; these new needs have stimulated three new areas of research: technology with the development of new methods for fabricating fluidic systems, applied research with the development of components from which functionally complex fluidic devices can be assembled, and fundamental research with the examination of the behaviour of fluids in small channels. Developments in microfluidics technology are also contributing to new experiments in fundamental biology, materials science, and physical chemistry.

Unlike microelectronics, in which current emphasis is on further reduction of the size of components, microfluidics is focusing on making more complex systems of channels with more sophisticated fluid-handling capabilities, rather than reducing the size of the channels; microfluidic systems require the same types of components as larger fluid-handling systems: pumps, valves, mixers, filters, separators, and the like. Although the

size of channels is still large relative to the size of features in microelectronic devices, they are so small that flows behave quite differently than the large-scale flows that are familiar from everyday life. The components needed at small scales, dealing with volumes of fluid ranging from microliters down to picoliters are therefore often quite different from those used at large scales.

Microfluidics hardware requires special design and fabrication considerations different from macroscale devices; i.e. it is not possible to conceive a conventional fluidic system, scale down the dimensions and then expect it to function in microfluidic applications. When the dimensions of a device or a system become smaller, the behaviour of the fluid is dramatically altered. Some effects negligible on the macroscale, could become dominant on the microscale, for example capillarity action changes the way fluids pass through a tube with a diameter less than one millimetre whereas it does not influence the way the fluid flows through a large tube.

The main challenge in microfluidics is to control these differences of behaviour and, even better, to find a way to take advantage of them.

The volumes involved in microfluidics can be understood by visualizing the size of a one-litre container, and then imagining cubical fractions of this container. A cube measuring 100 mm edge has a volume of one litre. Imagine a tiny cube which height, width, and depth are 1/1000 (0.001) of this size, or 0.1 mm. This is the size of a small grain of table sugar; it would take a strong magnifying glass to resolve it into a recognizable cube. That cube would occupy 1 nL. A volume of 1 pL is represented by a cube which height, width, and depth are 1/10 (0.1) that of a 1 nl cube. It would take a powerful microscope to resolve that.

Microfluidic systems have diverse and widespread applications. Some examples of systems that employ this technology include inkjet printers [1],

[2], blood-cell-separation equipment [3]-[6], biochemical assays [7], [8], chemical synthesis [9]-[13], genetic analysis [14]-[16] and drug screening [17]-[19]. About the processes involved I the fabrication there are surface micromachining, laser ablation, and mechanical micromilling. The use of microfluidic devices to conduct biomedical research and create clinically useful technologies has a number of significant advantages: for example because the volume of fluids within these channels is very small, usually a few nanoliters, the amount of reagents and sample used is quite small. This is especially significant for expensive reagents and for forensic analysis, where only small sample volumes are often available. The fabrication techniques used to construct microfluidic devices, discussed in more depth in next chapters, are relatively inexpensive and also allow mass production. In a manner similar to microelectronics, microfluidic technologies enable the fabrication of highly integrated devices with different functions on one substrate chip. One of the long term goals in the field of microfluidics is to create integrated, portable clinical diagnostic devices for home and bedside use, thereby eliminating time consuming laboratory analysis procedures; for these reasons, not surprisingly, the medical industry has shown a keen interest in microfluidics technology.

1.1.1 Basic principles of microfluidics

When a fluid gets inside a pipe or in a channel the flow can show different behaviours in dependence of physical properties, flow rate and geometry of the system; basically it is possible to define two typologies of flux: laminar and turbulent.

Laminar flux is characterised by parallel flow lines without any interference between each other; oppositely, if the flow lines are not parallel and they have some intersection or if there is a formation of vortex, the flow is called turbulent. In a turbulent regime there is mass transfer in the direction perpendicular to the wall of the channel, and this allows phenomena as mixing or heat transfer to be enhanced.

A parameter that can give information about the characteristic of the flow in a pipe or channel is the Reynolds number, R_e, and is defined as:

eq. 1 $$R_e = \frac{Lvr}{m}$$

where μ is the viscosity, ρ is the fluid density, and v is the average velocity of the flow, L is a length scale and is equal to 4A/P where A is the cross sectional area of the channel and P is the wetted perimeter of the channel. Due to the small dimensions of microchannels, the R_e is usually much less than 100, often less than 1.0. In this Reynolds number regime, flow is completely laminar. The transition to turbulent flow generally occurs at a Reynolds number larger than 2000. Laminar flow provides a means by which molecules can be transported in a relatively predictable manner through microchannels. Note, however, that even at Reynolds numbers below 100, it is possible to have momentum-based phenomena such as flow separation. In the long, narrow geometries of microchannels, flows are also predominantly uniaxial: the entire fluid moves parallel to the local orientation of the walls. The significance of uniaxial laminar flow is that all transport of momentum, mass, and heat in the direction normal to the flow is by molecular

mechanisms: molecular viscosity, molecular diffusivity, and thermal conductivity.

The flow of fluid through a control volume can be described by the Navier-Stokes equations. These equations can be derived from the principles of conservation of mass, momentum and energy. The equation for the conservation of mass states that at all times (for incompressible, steady flow) the mass entering the control volume is equal to the mass leaving the control volume,

eq. 2 $$\frac{\partial r}{\partial t} + \nabla \cdot (rn) = 0$$

where ρ is the fluid density, t is time and v is the local fluid velocity. This equation is also often called the 'continuity equation' because it is based on the assumption that the fluid medium is continuous.

As an analogue to Newton's second law of motion, the conservation of momentum equation states that the change in momentum within the control volume is equal to the sum of the forces acting on the control volume,

eq. 3 $$\frac{\partial (rn)}{\partial t} + \nabla \cdot (rnn) = -\nabla P + (\nabla t) + rg + F$$

where P is the pressure, τ is the viscous stress, g is the gravitational body force and F is any other body force.

As already mentioned in this chapter, in a microfluidic context some effects that can become important or dominant, although in a macroscopic system

they can be totally neglected. One of these effects that can play a fundamental role is the capillary action.

1.2 Capillarity

Capillarity is defined as the movement of liquids within the spaces of a porous material or a capillary due to the forces of adhesion, cohesion, and surface tension. For example, the upward flow of liquid by capillary action is essential to the maintenance of a candle flame. Radiant heat from the candle flame melts the wax at the base of the candle wick. The molten wax is drawn upward in the wick by capillary action, evaporating as it rises because of heat transfer from the flame surrounding the wick. The vapour then diffuses into the flame, burning by mixing with the surrounding air and feeding back some heat to maintain the process of melting and evaporation.

Another interesting example of capillary action is represented by the vegetal world: plants' roots in the soil are capable of carrying water from the soil up into the plant. Water, which contains dissolved nutrients, gets inside the roots and starts mount in the plant tissue. As water molecule #1 starts climbing, it pulls along water molecule #2, which, of course, is dragging water molecule #3, and so on; so plants and trees could not thrive without capillary action.

1.2.1 Wettability and contact angle

An important characteristic of a liquid is its ability to wet a surface. At the liquid-solid surface interface, wetting of the surface occurs when the adhesive forces are stronger than the cohesive forces, in other words when

molecules in the liquid have a stronger attraction to surface molecules of the solid than to each other. Alternatively, if the liquid molecules are more strongly attracted to each other and this effect prevails over the attraction to the solid surface (the cohesive forces are stronger than the adhesive forces), then the liquid beads-up and does not wet the surface. One way to quantify a materials' surface wetting characteristic is to measure the contact angle of a drop of liquid placed on the surface of the material. The contact angle, $?_c$, is the angle formed by the solid/liquid interface and the liquid/vapour interface, measured from the side of the liquid. Figure 1-1 shows some of the possible wetting behaviours of a drop of liquid placed on a horizontal, solid surface.

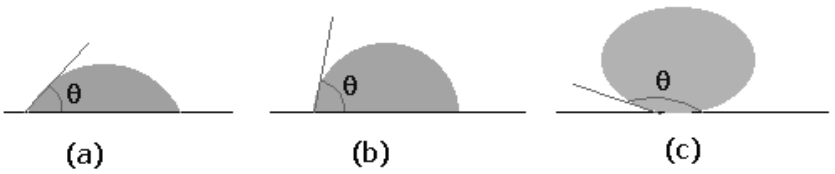

Figure 1-1 contact angle

Figure 1-1(a) represents the case of a liquid which wets a solid surface well, e.g. water on clean copper.

Figure 1-1(c) represents the case of no wetting. If there were exactly zero wetting, $?_c$ would be 180^o. However, the gravity force on the drop flattens the drop, so that 180^o angle is never observed. This might represent water on Teflon or mercury on clean glass. For perfect wetting, in which the liquid spreads as a thin film over the surface of the solid, $?_c$ is zero. Figure 1-1(b) represents an intermediate wetting.

It is normally said that a liquid wets a surface if $?_c$ is lower than 90^o and does not wet if $?_c$ is larger than 90^o. Values of $?_c$ lower than 20^o are considered strong wetting, and values of $?_c$ higher than 140^o are strong nonwetting.

The wetting ability of a liquid is a function of the surface energies of the solid-gas interface, the liquid-gas interface, and the solid-liquid interface. The surface energy across an interface or the surface tension at the interface is a measure of the energy required to form a unit area of new surface at the interface. The intermolecular interactions or cohesive forces between the molecules of a liquid cause surface tension. When the liquid encounters a solid substance, there is usually an interaction between these two. The adhesive forces between the liquid and the other substance will compete against the cohesive forces of the liquid. Liquids with weak cohesive bonds and a strong attraction to the solid material will tend to spread.

Liquids with strong cohesive bonds and weaker adhesive forces will tend to bead-up or form a droplet when in contact with the second material. In liquid wetting tests, there are usually three interfaces involved, the solid-gas interface, the liquid-gas interface, and the solid-liquid interface. For a liquid to spread over a surface, two conditions must be met: first, the surface energy of the solid-gas interface must be greater than the combined surface energies of the liquid-gas and the solid-liquid interfaces; second, the surface energy of the solid-gas interface must exceed the surface energy of the solid-liquid interface.

The wetting characteristics of a liquid are also largely responsible for its ability to fill a void. Fluids are often pulled into surface breaking defects by capillary action. The capillary force driving the liquid into the crack is a function of the surface tension of the liquid-gas interface, the contact angle, and the size of the defect opening.

1.2.2 Capillary action

Capillary action is a phenomenon in which the surface of a liquid is observed to be elevated or depressed where it comes into contact with a solid. For example, the surface of water in a clean drinking glass is slightly higher at the edges, where it is in contact with the glass, than in the middle, as shown in Figure 1-2. Capillarity can be explained by considering the effects of two opposing forces: adhesion, the attractive (or repulsive) force between the molecules of the liquid and those of the container, and cohesion, the attractive force between the molecules of the liquid. Adhesion causes water to wet a glass container and thus causes the water's surface to rise near the container's walls. If there were no acting forces opposing these adhesion forces, the water would creep higher and higher on the walls and eventually overflow the container. The forces of cohesion act to minimize the surface area of the liquid; when the cohesive force acting to reduce the surface area becomes equal to the adhesive force acting to increase it (e.g., by pulling water up the walls of a glass), equilibrium is reached and the liquid stops rising where it contacts the solid. In some liquid-solid systems, e.g., mercury and glass or water and polyethylene plastic, the liquid does not wet the solid, and its surface is depressed where it contacts the solid.

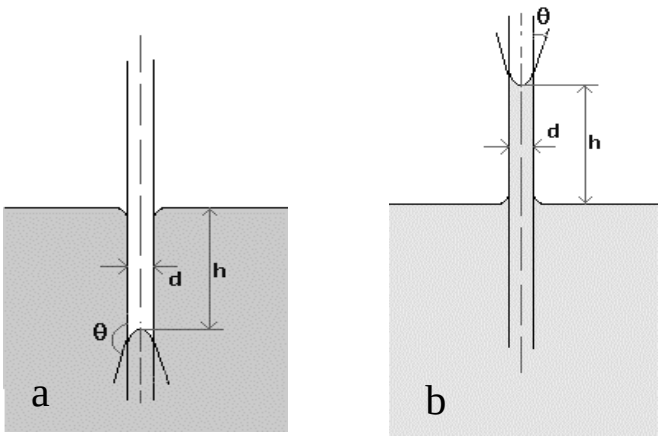

Figure 1-2 capillarity effect in an hydrophobic (a) and hydrophilic capillary (b)

Capillarity is pronounced when using tubes smaller than about 10 mm in diameter.

Capillary rise (or depression) in a tube can be calculated by making force balances. The forces acting are the force due to the surface tension (F_s) and due to the gravity (F_g).

The force due to surface tension,

eq. 4 $$F_s = \pi d \sigma \cos(\theta)$$

where d is the diameter of the capillary, s the surface tension and θ is the wetting angle or contact angle.

This is opposed by the gravitational force acting on the column of fluid, and it is equal to the height of the liquid above (or below) the free surface and is expressed as

eq. 5 $$F_g = (\pi/4) d^2 h g \rho,$$

where ρ is the density of liquid, h the height of the liquid column and g the gravitational acceleration.

Combining these forces and solving for the height of the liquid column, we find

eq. 6 $$h = 4\sigma \cos(\theta) / (\rho g d).$$

This last equation expresses the relation between the liquid column and the physical parameters of the liquid itself and the geometry of the system.

1.3 Lab-on-chip

1.3.1 Introduction

The possibilities that are envisioned by using microfluidic systems have not only interested scientists, but also industries, especially from the Life Sciences (food, medical, biotech) and fine chemistry (pharma). Microfluidics is a discipline that makes use of MEMS (Micro-Electro-Mechanical-Systems) in which minute quantities of liquids or gases are manipulated, monitored, analyzed, and even processed. Microfluidics based instruments are capable of synthesizing and analyzing (bio)chemical materials at a very high throughput and against relatively low costs. These decisive benefits are enabled by the reduced consumption of reagents, short analysis times, faster mixing, and the high degree of automation possible compared to conventional equipment. Referring to the size of microfluidics based systems, they are often called Lab-on-a-Chip systems.

1.3.2 Approaches of Lab-on-a-Chip

Roughly, one can distinguish two main areas in Lab-on-a-chip based systems. In the first place there are the so-called biochips of glass or polymer, which have passive fluidic functions and which are being applied in combination with bulky laboratory equipment providing functions such as sample and reagent supply, high voltage control for electro-osmotic pumping, and optical (fluorescence) detection. On the other hand, there is the emerging area of true lab-on-a-chip systems, in which all, or at least the main, functions are combined in a complete (sub)system (Figure 1-3). Somewhere in-between are the so-called micro-arrays having an integrated

detection function and which can be applied in combination with a desktop apparatus, for such as sample preparation and supply.

Figure 1-3 **e*xample of a Lab-on-Chip device: Agilent 2100 Bioanalyzer, together with its Cell Assay Extension, can perform simple flow-cytometric analysis.***

These revolutionizing Lab-on-a-chip equipments are introduced rapidly. In pharmacy and genomics, for example, experiments can be performed by thousands in parallel resulting in more efficient discovery of new drugs and the accelerated unravelling of the human genome (high throughput screening). In fine chemistry, the optimization of process parameters and production of small quantities are performed in the very same system, bypassing the expensive scaling up stage (process-on-a-chip). Other emerging applications are in medical, clinical and further analysis instrumentation. The number of possible applications for a quick, cheap and portable analysis of any liquid or gas sample is beyond imagination; it can give the information technology world electronic taste and smell, it can

monitor water quality on line everywhere, check for alcohol or drugs in blood or breath on the spot etcetera.

The interest for decentralised analysis first emerged for clinical laboratory testing and reports of miniaturised integrated analytical test cartridges were made as early as in the 1970's[20], [21]. Introduced in the 1990's, the micro total analysis system (μTAS) concept formalised this "lab-on-a-chip" approach by describing miniature platforms offering the functionality of a complete bench top analysis system [22], [23], [24]. Since then, considerable research effort has been devoted to miniaturising sampling, sample pre-treatment, separation and detection for a variety of applications in drug discovery, genomics, clinical diagnostics, environmental and eventually food analysis.

The viability of μTAS depends in part on the development of miniature fluidic components, such as pumps and valves, mixers, filters [25], [26]. A number of fine engineering techniques have been exploited to this end. Those originating from the semiconductor industry are based upon pattern transfer by photolithography and bulk micromachining of silicon, quartz or Pyrex [27]. Monocrystalline silicon can in particular be etched anisotropically in a proper etching solution as a result of a strong crystallographic dependence of the etch rate. Characteristic etch profiles can be generated to produce simple microfluidic devices. Machining precision and design flexibility can be improved by using deep reactive ion etching (DRIE), which offers the advantage of a directional etch but independently of the crystal orientation. Aspect ratio (defined as feature width to engraved depth) up to 1:15 can be achieved, which opens a number of opportunities for the design of reactors, optical cells and sampling devices. Alternative materials and methods include replication techniques based on plastics, used for instance

by the compact disk industry [29]. Replication techniques are based upon the transfer of a surface-relief profile from a master surface into a formable material such as a thermoplastic or a curable polymer. It includes hot embossing, casting and injection moulding. These technologies are particularly well suited for a low-cost and mass production of microstructures. Average cost per cm^2 is the lowest for roller hot embossing, followed by stamp embossing, casting and injection moulding.

1.4 CREAM project

Consumer's rising concern on healthy food and environmentally sound production methods has set new technological challenges in food production. Quality management in the food chain to ensure product safety includes the monitoring of potential residues of pesticides, veterinary drugs and other chemical compounds. These residues can be found at different concentration levels in products from animal origin, such as milk or meat. In the case of antibiotics, residues may "simply" inhibit starter cultures in the production of yogurt, cheese and other solid milk products, and affect the quality of these. More importantly, antibiotic residues may have in the long term a potential insidious effect on public health.

Until now, the analysis or detection of these substances is most commonly performed using microbiological methods and physical-chemical High Performance Liquid Chromatography (HPLC) methods in the post-screening phase. There are disadvantages to this approach as these tests can only be performed in a well-equipped laboratory. Aside from the fact that

this approach is costly, there is a tendency to bring the "laboratory to the samples", that is to identify certain critical points in the production chain and perform the control directly at these points: e.g. production chain management, hazard analysis critical control points (HACCP). To make this a feasible approach, simple and cheap devices for on-site monitoring of critical parameters are needed. A large part of the work reported in this thesis has been done in the frame of the project CREAM. The project objective was to develop and optimize an analytical cartridge supporting a molecularly imprinted polymer assay for on-site monitoring and discrimination of ß-lactam residues in milk. The ß-lactam antibiotics of the penam type (benzylpenicillin, ampicillin, amoxicillin etc.) are often used to treat mastitis, the inflammation of the cow's udder, which is a very frequent and severe problem in farming. The milk industry is highly interested in automated, quick and sensitive tests for ß-lactam antibiotics because these substances may inhibit, even at trace levels, the fermentation processes of milk for cheese and yogurt production. The entire analytical procedure should ultimately be carried out within the cartridge to offer straightforward and reliable analyses.

1.4.1 Project objectives

To meet the need of alternative confirmatory methods and practical instrumentation for on-site monitoring and discrimination of β-lactam residues in milk, the main objective of the project was to develop and optimise a plug-in detection cartridge supporting a molecularly imprinted polymer assay. This cartridge will consist of a microfabricated column (or, in alternative, a chamber) accommodating an optical detection window.

Molecularly imprinted polymers (MIPs) in the form of beads will be used as packing material and recognition elements. Often reported as plastic antibodies, MIPs are usually cheaper and more robust than their biological counterparts. This material is remarkable for the discrimination of target molecules and well adapted for the analysis of real samples. These beads will act as a stationary separation and preconcentration phase. The assay will be specifically developed for the screening of β-lactam marker residues in a flow analysis system. Analyte binding will be detected by fluorescence means to meet the targeted assay characteristics. Different assay formats, labels and optical detection schemes have to be evaluated and the best candidates optimised to meet the required assay specificity and sensitivity. Detection of penicillin antibiotics and their residues in milk has been chosen as a relevant and practically important model system. Participation of a national reference laboratory in the project can allow field trials of the developed cartridge in real experimental conditions and validation of the analytical method. Further project objectives are directed to the development and optimisation of the technical means that are necessary to achieve the main objective:

- Development of a cartridge support for molecularly imprinted polymer assays (MIAs).
- Development and optimisation of MIPs for the targeted assay specificity and sensitivity.
- Synthesising and characterisation of the appropriate fluorescent labels.
- Evaluation and selection of the best assay format for the MIA.
- Production of MIPs in a suitable format for implementation in the cartridge.
- Definition and optimisation of the optical detection scheme.

- Design of a cartridge allowing easy handling and quick part replacement.
-Implementation of a cartridge fabrication process amenable to industrial production.
- Development of the appropriate instrumentation in a portable set-up.
- Development and optimisation of the overall analytical procedure.
- Demonstration of multi-residues detection.

1.4.2 Cartridge design and identification of the functionalities

Both the developments of the MIA and of the cartridge were concurrent. Initial assumptions were made and the operational and technical requirements of the assay defined. It was assumed that a number of operations preceding the β-lactams detection would be necessary and the following steps were identified:
- Sample milk
- Add and mix with reagents
- Precipitate milk proteins
- Filtrate particles (curd) to obtain a homogeneous solution for the optical detection
- Pre-concentrate β-lactams on the MIPs
- Elute (in the case of a competitive assay)
- Detect optically

During the development of the imprinted polymers it appeared that the recognition process of the target analyte would only be effective in the exact solvent composition used during the imprinting process. MIP materials, as the ones developed in the CREAM project, have selectivity for the β-lactam only when a solvent composition containing a low amount of water is used,

typically 1-2% of water. Effectively, the milk samples need to be either diluted 50-100-fold in acetonitrile to achieve the appropriate conditions for selective sorption, or dehydrated. Whereas dilution can technically be done within the cartridge, it significantly increases the volume of the sample and will cause incomplete sorption. Indeed, a sensitive detection of the analytes has been observed with low volumes of a few millilitres applied to MIP columns.

1.4.3 Molecular Imprinted Polymers

The most promising material in the field of artificial molecular recognition systems are molecular Imprinted Polymers (MIPs). The MIPs necessary for the final cartridge were developed by a project partner (Department of Pure and Applied Biochemistry, Lund University, Sweden). Molecular imprinting technologies offer advantages by providing polymers capable of molecular recognition and catalysis, which can be used in conjunction with chromatographic separations, chemical sensing or catalytic reactions performed in different organic solvents. The concept behind this technique involves moulding material (with the desired chemical recognition properties) around individual molecules (template). Upon removal of the molecular template, the material retains its moulded shape to fit and coincide with that of the template molecules. It is well known from both biology and chemistry that molecules tend to stick to receptors or surfaces with complementary shape, i.e. the “lock and key” theory of enzymes. Thus, molecular imprinting results in materials that can selectively bind to molecules of interest.

Recent years have seen increased interest in molecular imprinting technology [39], also reflected in several review [40]-[43] that emphasized the application of MIPs in chromatography separation. Concerning chemical sensing there is an exhaustive review of MIPs and their use in biomimetic sensors [41] and also in optical sensing [42], an area showing the most important applications of MIPs within the chemical sensing field.

Molecular imprinting is a versatile technique that allows preparation of materials that contain specific recognition sites (for binding or catalysis) with a shape and geometry of functional groups complementary to those present in the template molecule. One of the most popular methods of producing MIPs is bulk polymerisation [43], in which functional monomers are bound either covalently or non-covalently to a print molecule or template. The correct positioning of these functional groups allows them to converge on the template molecule in a reciprocal fashion. The resulting pre-polymer complex is copolymerised with an excess of cross-linking monomer in the presence of an equal volume of inert solvent and a free radical initiator. Polymerisation of this mixture results in a highly cross-linked insoluble polymer. Removal of the template, in most cases by extraction or hydrolysis, leaves sites complementary in size and shape to the template molecule, resembling the “lock and key” model of enzyme. The block of polymer is then ground and sieved in order to produce imprinted receptor particles of appropriate size. MIPs have been applied to the development of piezoelectric and electrochemical sensors and in radioactive competitive assays.

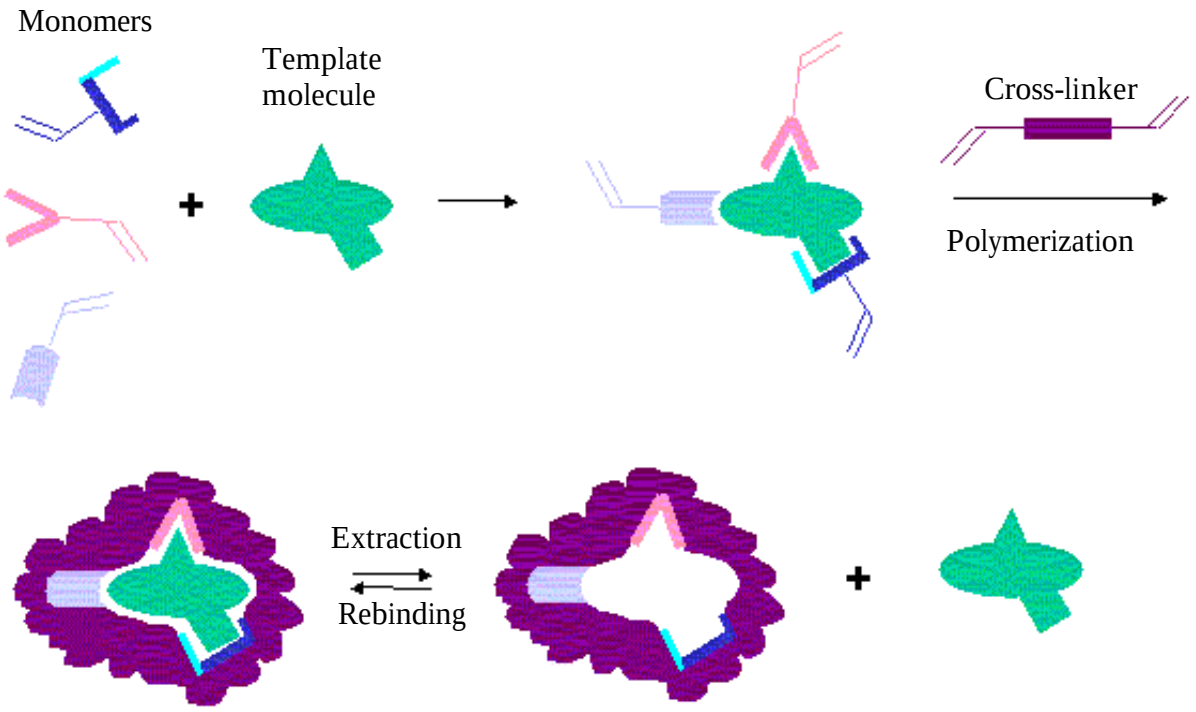

Figure 1-4 schematic representation of the molecular imprinting process

However, its application to optical sensors is still limited due to the lack of appropriate fluorescent molecules able to compete with the template by specific binding sites in the polymer. Optimisation of the polymer composition to get the maximum specific binding in the last time is another aim of research of this area.

1.4.4 The CREAM cartridge

The complete description of the cartridge developed in the project CREAM is presented in the chapter 6, and it results from the integration of different microfluidic elements developed during this work. The components that find place in this cartridge are a microreactor, a sample metering system and

an optical detection cell. In order to manage the fluid inside the cartridge a set of stop fluid valves is inserted between the microfluidic elements, the development of such a valve is described in chapter 4. All the components developed during this work are individually characterised in their microfluidic functionalities as well as upon integration in the cartridge; in spite of that, direct measurements of antibiotic in milks have not been possible in the project time limits.

2 Fabrication methods

2.1 Introduction

Microfabrication or micromachining in the narrow sense comprises the use of a set of manufacturing tools based on batch thin and thick film fabrication techniques commonly used in the electronics industry. In the broader sense, microfabrication describes one of many precision engineering disciplines which take advantage of serial direct write technologies, as well as of more traditional precision machining methods, enhanced or modified for creating small three-dimensional structures with dimensions ranging from millimeters to submicrometers, involving sensors, actuators, or other microcomponents and microsystems.

Both micromachining and microelectronic fabrication start with photolithography, the technique used to transfer copies of a master pattern onto the surface of a solid material, such as a silicon wafer.

After photolithography succeeded, a number of subtractive and additive processes are performed; materials are either removed from, or added to a substrate, usually in a selective manner. The processes used are borrowed from conventional integrated circuitry and thin film manufacturing, transferring the lithography patterns to the surface structures or three-dimensional micromachines.

This chapter deals both with photolithography and etching techniques used for the realisation of the devices described in next chapters.

2.2 Photolithography

Lithography is the technique used to transfer copies of a master pattern on to the surface of a solid material, the term of photolithography is used when the copy is transferred with the help of the light. In this process a silicon wafer coated with a thin film of photoresist is selectively exposed to ultraviolet light. The mask used for the selective exposition is a transparent quartz frame that contains opaque chromium regions representing the geometry needed to be transferred to the photoresist. Photoresists are resins that can be made soluble (positive photoresist) or insoluble (negative photoresist) upon exposure to ultraviolet light. After exposure the photoresist is developed by dissolving the unwanted part. After the photolithography, photoresist acts as a mask during the etch of silicon oxide or silicon.

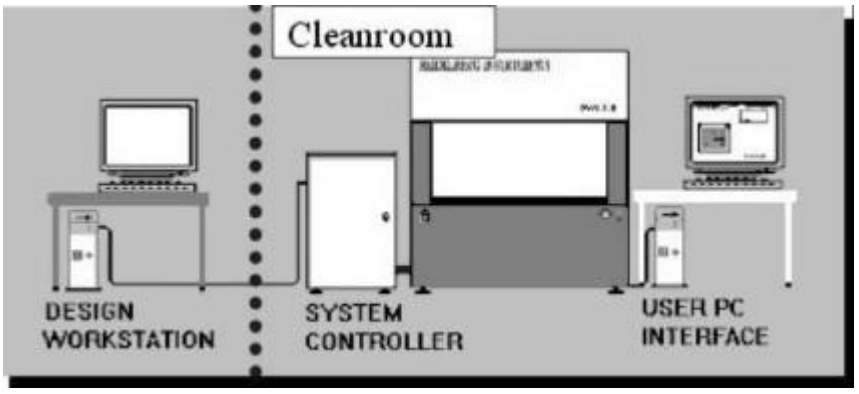

Figure 2-1 schematic representation of the chromium mask writing setup.

The masks necessary for the realisation of the devices described in this thesis have been designed using the layout software CleWin (WieWeb Software, Hengelo, The Netherlands); with a laser writer Heidelberg DWL200 at the EPFL (Ecole Politechnique Féderal de Lausanne). The chromium masks are provided with the photoresist coating. Then the photoresist is developed,

the chromium etched and finally the mask is cleaned to remove the remaining photoresist.

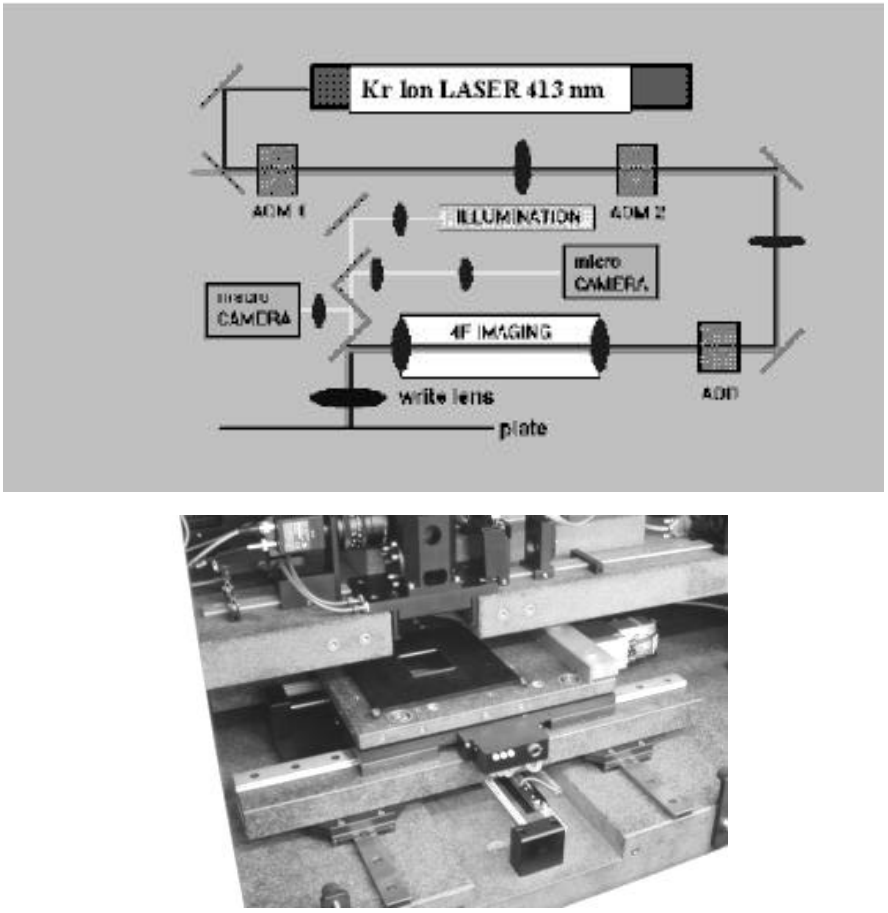

Figure 2-2 schematic representation of the optical system used to write chromium masks and a picture of a chromium mask during the writing

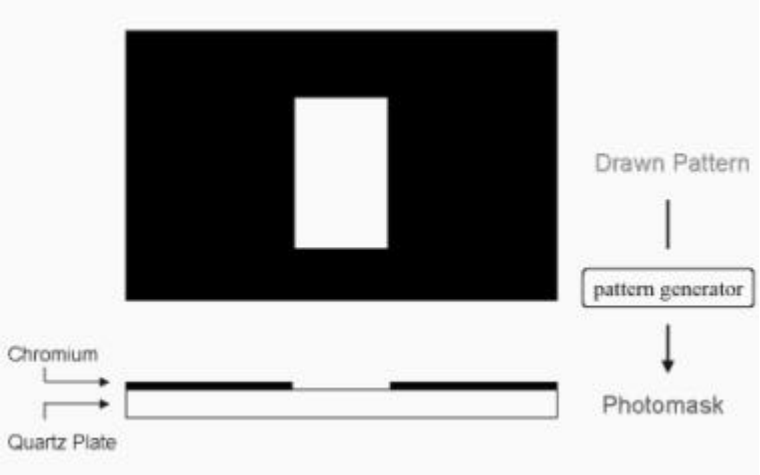

Figure 2-3 schema of a chromium mask production

For the realisation of the devices described in next chapters, before starting the photolithographic process on silicon substrate, an often common step is the growth of a thin layer of silicon oxide on the surface by heating the wafer at temperatures between 900 and 1150 ^{o}C in a steam or in a humid oxygen steam. After oxidation, and in order to increase resist adhesion, the wafer is first dehydrated in an oven under air at 200 ^{o}C for about 30 minutes, then the surface is reacted with gaseous hexamethyldisilazane (HMDS), which modifies the surface with a monolayer of trimethylsilane-groups.

The photoresist, a viscous solution of the monomer, solvents and photoinitiator, is dispensed on to the wafer, which is then spun at high speed, between 1500 and 4000 rpm depending on the viscosity and the required thickness. The choice of photoresist depends on its role in the next fabrication steps, in this work two positive photoresists have been used: the AZ1518 and AZ4562 (Clariant, Muttenz, Switzerland). The first one allows thickness of about 7μm, and is used to produce the mask for wet oxide etching in BHF. For DRIE the second resin is preferred because it allows thicker layer deposition (about 13 μm). After spin-coating, the resist still contains up to 15% of solvent, therefore the wafer is baked at 100 ^{o}C to remove solvents (pre-bake).

After the pre-bake, the resist coated wafer is transferred to the mask aligner, the exposure system, where the mask is inserted. In this system the mask is between the light source and the wafer, and that allows the selective illumination of the substrate making soluble the exposed photoresist.

Development transforms the latent resist image formed during exposure into a relief image which serves as a mask for the further fabrication steps.

Finally, before etching, the resist needs a post-bake, in order to remove residual developer or solvents, and also to improve the hardness of the film increasing the resistance of the resist to subsequent etching steps.

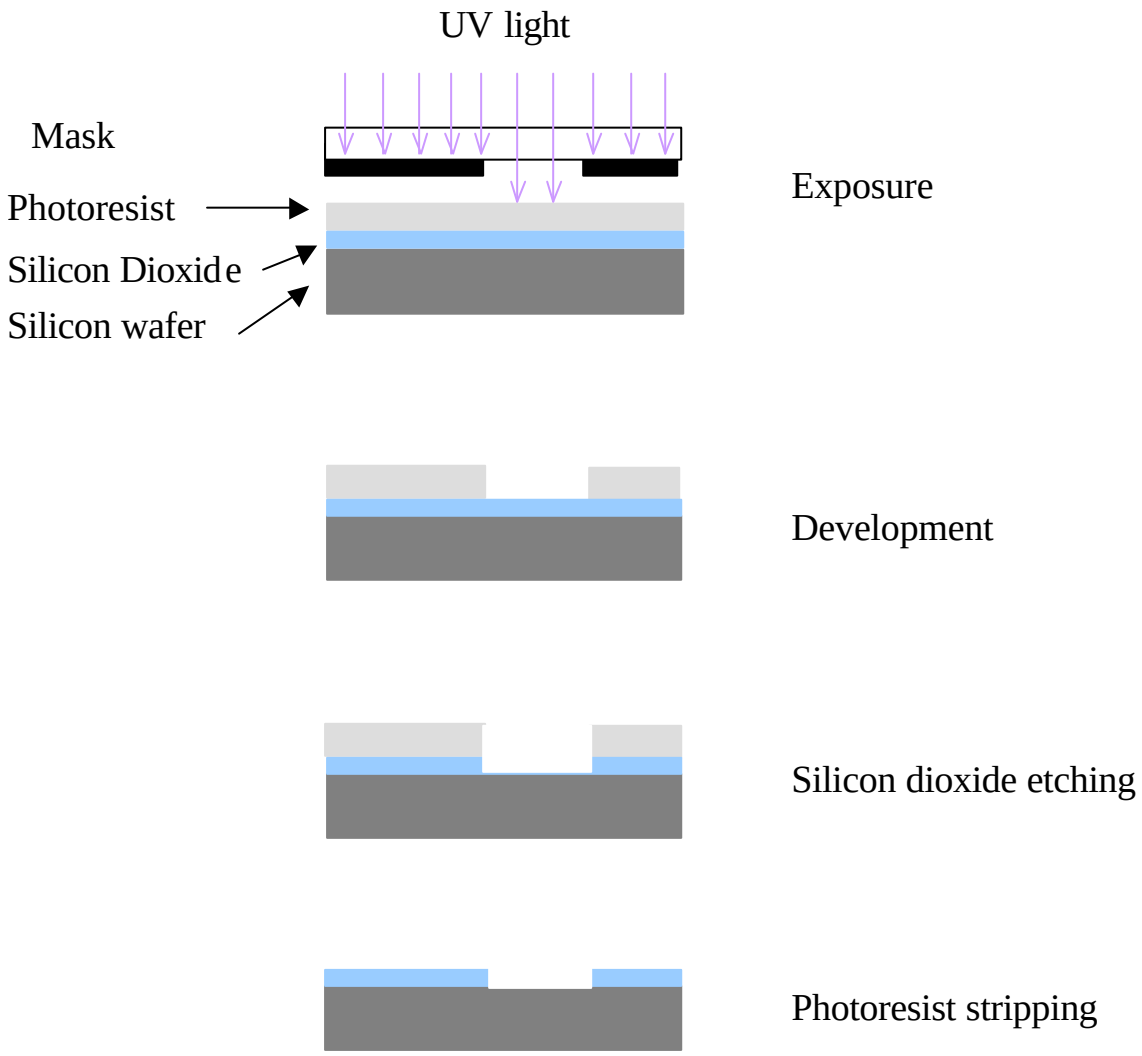

Figure 2-4 sequence of the photolithography steps

For the realization of three dimensional micro structures with photoresist Epon SU8, a negative photoresist, can be used that allows the fabrication of high aspect ratio micro structures and can be coated in thicknesses of up to 1200 µm. During this work SU8 had been used to make masters for the realisation of microfluidic devices using plastic replication techniques, described later in this chapter.

2.3 Silicon dioxide wet etching and Deep Reactive Ion Etching (DRIE)

Photoresist is used as an etch mask that delineates the pattern geometry and protects the underlying film. Usually etching processes are subdivided in two categories: wet and dry etching.

Wet etching can be simply described as the dissolution of the material in the appropriate etchant, the resist must be resistant to the etchant in order to provide a good protection throughout the patterning process.

Silicon dioxide is etched in a buffered hydrofluoric acid solution (BHF) at room temperature. BHF consists of 7 parts of 40% NH_4F and 1 part of HF and has typical etching values in the order of 800 Å/min.

Concerning the possibilities of silicon etching, they changed drastically with the advent of the currently available DRIE tools; this dry processing technique permits the fabrication of high aspect ratio silicon structures without limitation in geometry. The etching procedure is an alternation of isotropic silicon etching and passivation of the sidewalls during the next etching step. More precisely, after the masking material (photoresist or silicon dioxide) has been patterned, a shallow isotropic trench is formed, in the subsequent passivation step a protective film is deposited everywhere. During the next etch step the protective film is removed from all horizontal surfaces by directional ion bombardment, and another shallow trench is formed. This high-density plasma tool in which the etching and passivating gases are introduced in the reaction chamber independently one at time (as represented in Figure 2-5). The machine alternates between an etching cycle and a passivating cycle in the so called time-multiplexing scheme, TMDE. It

is also possible to have a standard approach in which all gas species are present at same time.

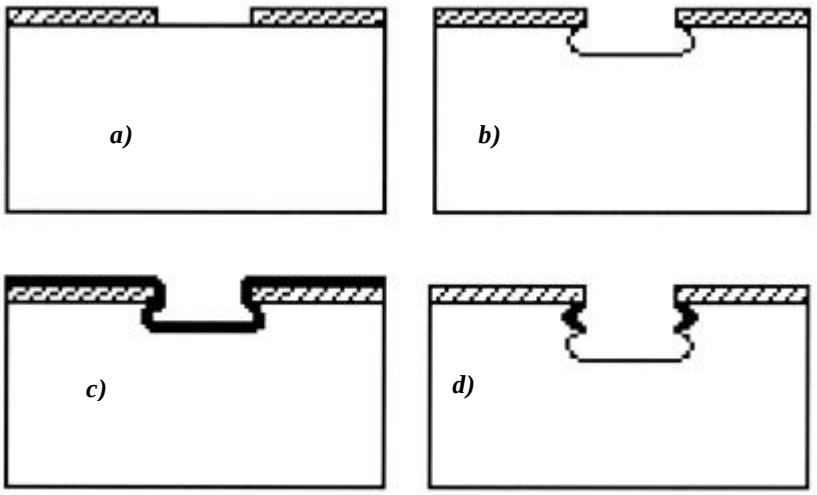

Figure 2-5 schematic representation of sequential steps during TMDE; a)patterning of the masking material, b) formation of a shallow isotropic trench, c) passivation step, d) an other shallow trench is etched.

2.4 Plastic replication

During this work a method to reproduce in plastic a device from a silicon master has been developed. After having tested several replication techniques it was found that the most satisfying one is by cast-moulding. This technique, shown in Figure 2-6, consists of the fabrication of a master, a first replication in silicone rubber to produce the mould that is subsequently used to make the replication of the master in plastic.

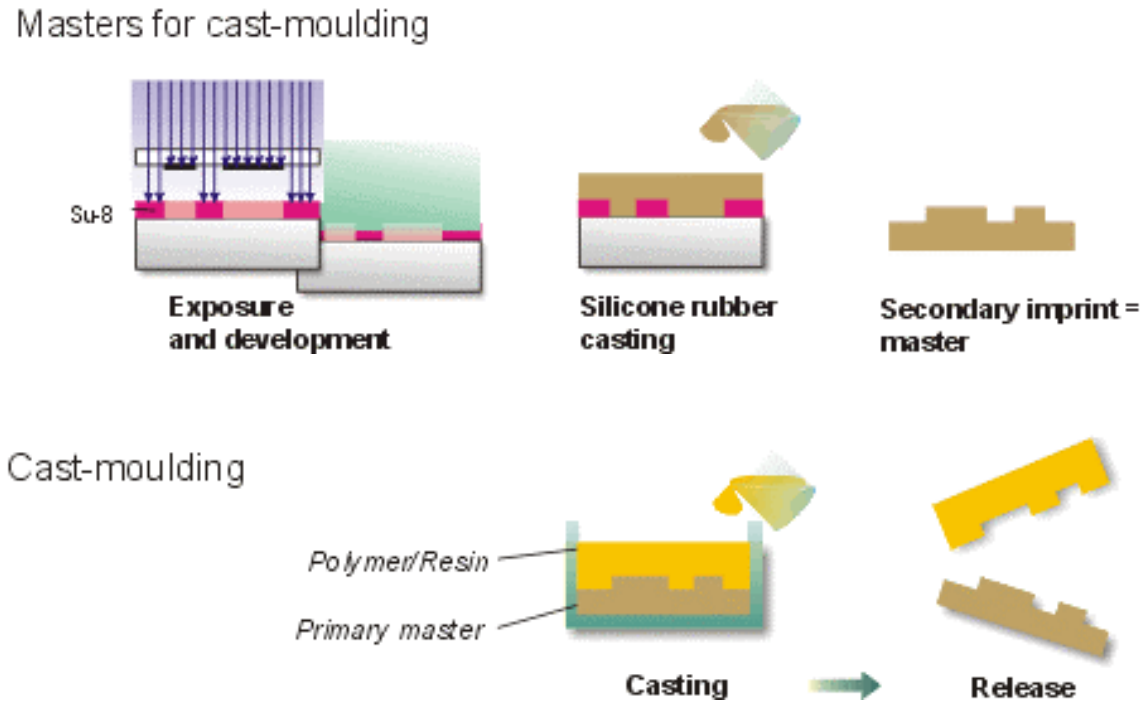

Figure 2-6 steps for plastic replication by cast-moulding

The master for cast-moulding is produced in Epon SU-8 by photolithography. Starting material was a 4" silicon wafer, 535 µm thick with no special requirement on the crystal orientation. Wafers were first thermally oxidized to produce a thin protective coating of 200 nm. SU-8 was then spin coated on the wafer and patterned by UV light using a conventional mask aligner. Photomasks most simply consisted in a printed acetate foil when feature sizes below 7 µm were not needed. A regular chromium mask was used for better resolution. The wafer was diced into individual master chips. A first imprint was obtained by casting silicone rubber (Rhodorsil RTV 585). This primary imprint was further used to cast mould a mixture of epoxy resin Epon 825 and Jeffamine D-230 to produce stiffer replicas. The finest feature sizes produced in SU-8 were 25 µm (7.2 aspect ratio) and 50 µm (3.6 aspect ratio) with the chromium mask and the printed acetate foil, respectively. Note that the latter mask was not perfectly opaque and features obtained in SU-8 were approximately 30% larger than originally designed.

The proposed replication method is not restricted to SU-8, for instance Deep Reactive Ion Etching was used to generate the master for the percolation filter. Excellent pattern transfer from master to silicone imprints and ultimately to epoxy replica could be achieved. Steps of 1500 Å were revealed and even small irregularities induced by the printer pixels on the acetate foil could be observed on the final epoxy replicas. SU-8 masters could be used to generate 3 silicone primary imprints, from which 12 epoxy replicas could be made.

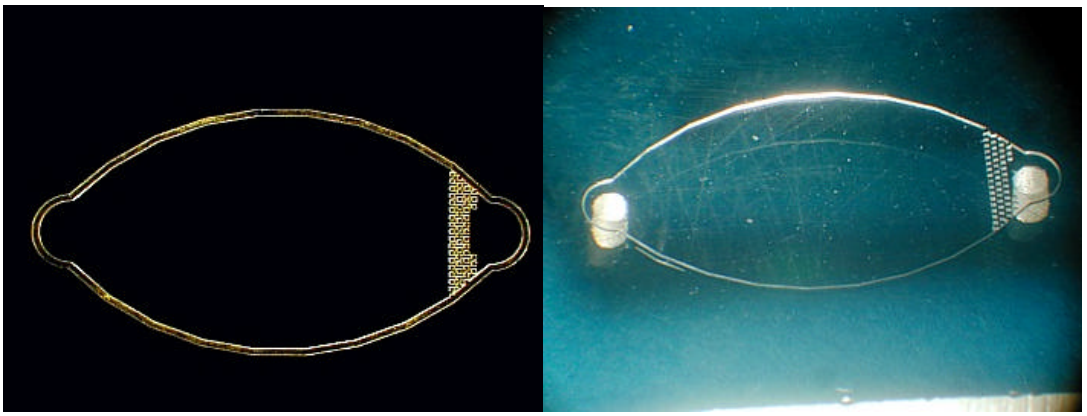

Figure 2-7 pictures of a master made in SU-8 (left) and the final structures in epoxy (right) - a packed-bed reactor

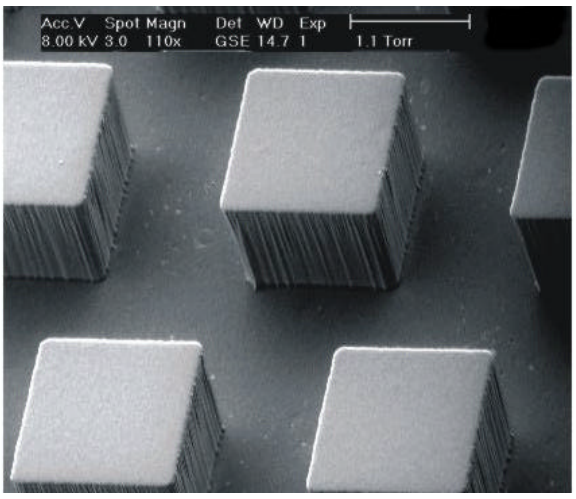

Figure 2-8 pictur of columns in EPON 825 by SEM (h´ L´ l 180´ 50´ 50 ㎜).

2.5 Devices assembly

In this paragraph techniques to assemble devices in silicon and pyrex, and plastic devices are explained. Basically two procedures have been used: anodic bonding and gluing with UV glue.

Concerning the first procedure, after processing the wafer in the clean room, it is diced to separate the different chips. A pyrex wafer is also diced into rectangles with the same dimensions as the silicon device, to make the lids closing the final chip. Several holes are drilled in pyrex to make fluidic connections between the holder and the channels etched in silicon. All the pieces are cleaned in a solution of sulfuric acid and hydrogen peroxide for about ten minutes, then rinsed in water and dried. Finally the chips are assembled in a sandwich pyrex-silicon-pyrex by anodic bonding. The pyrex lid is first bonded on top of the channels, the chip turned and the pyrex cover is bonded to the bottom.

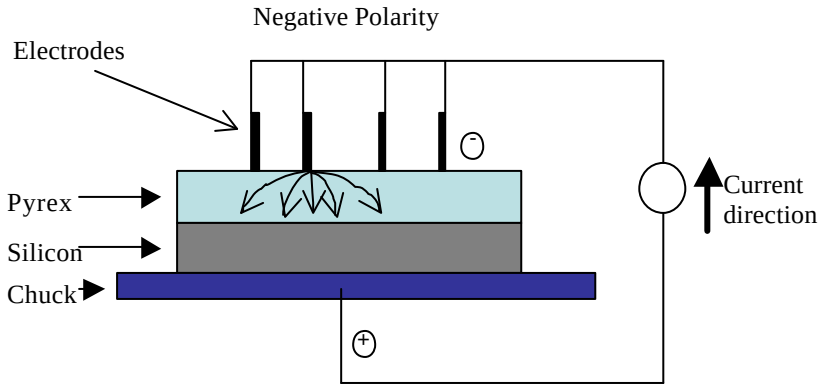

Figure 2-9 anodic Bonding setup

For anodic bonding, the working principle is to apply a large voltage potential across the glass-wafer system in order to generate an electric field that drives Na^+ ions in the glass wafer away from the interface region. Thus

a Na^+ depletion zone is formed and leaves oxygen molecules at the interface. Oxygen molecules then diffuse into the silicon to form a layer of amorphous SiO_2. The anodic bonding setup is shown in Figure 2-9.

The second technique is used to assemble plastic devices, in this case the two parts to be assembled are the device made in Epon 825 and the lid, usually in polymethyl methacrylate (PMMA), using a photosensitive glue. After the replication of the silicon wafer, the plastic replica is diced to have single devices, the fluidic connections are drilled and a lid in plexiglas made with the adequate dimensions. The two elements are put together under pressure and a few drops of glue are put at the interface between the two parts in plastic. By capillary effect the glue fills all the surface in contact between the two parts, without going into the channels. When the glue is uniformly distributed, it is exposed to ultra violet light to polymerise.

2.6 Conclusion

In this chapter all the techniques employed to fabricate the devices illustrated in the next sections have been described. All these technologies are based on well known microfabrication processes, but frequently they need some adaptations to be better suitable for the realisation of the specific devices.

3 Cartridge for ammonia detection

3.1 Introduction

Miniaturisation of chemical analysis and synthesis will improve throughput, performance and accessibility, and lead to significantly reduced costs. But experience has taught us that to maximise these benefits, it is not enough to work on the individual steps of a process (such as extraction, chromatography or detection), but it is necessary to scale down the entire system

As described in the first chapter, 'Lab-on-chip' technology is a rapidly growing research topic within the instrumentation and healthcare industries. The aim is to produce an automated, microscale laboratory to enable sample preparation, fluid handling, analysis and detection steps to be carried out within the confines of a single microchip.

For some applications the silicon-based fabrication technologies for these devices are being replaced with manufacturing technologies based on plastics and moulding. Plastic-based chips with integrated circuits are less expensive than their silicon counterparts, are easier to manufacture and handle, enabling the development of lower cost, more rugged and flexible devices.

In this chapter the basic steps for the realisation of a cartridge for the detection of ammonia are described, from its conception, through the development and realisation to final tests.

The devices described in this chapter are realised in plastic employing the cast-moulding method, described in paragraph 2.4, that basically consists in

three steps: fabrication of the master, production of a secondary imprinting in silicone rubber and final replication in plastic of the original master.
The master is fabricated in silicon and Epon SU-8 by photolithography, by casting silicone rubber on this first master a first imprinting is obtained which is then used to mould the resin Epon 825 to produce the final replica.
The chapter deals with the methodology to realise a cartridge for chemical analysis. Starting from the analysis of all the chemical steps performed in laboratory (i.e. sampling, mixing, time of reaction, detection), finding for each one a corresponding microfluidic element, realising all the single elements individually and test them in order to optimize their functionalities, integrating all the element in a monolithic device, as a cartridge, and testing the final device.

3.2 Chemical assay

Ammonia detection and measurement is a subject of interest in different fields from medical applications to the monitoring of fresh and marine water. Different techniques can be used to measure concentration of ammonia, such as laser based spectroscopy [44], amperometric [45], resistive or acoustic wave sensor [47] or fluorometric [46],[48]. In this work a technique based on fluorescence has been considered.
Ammonia reacts with OPA (orthophthaldialdehyde) in alkaline medium and in presence of thioglycolate to produce a fluorescent isoindole fluorophore. The optimum excitation and emission wavelengths for the fluorophore are respectively 370 nm and at 486 nm. A schematic view of the flow system used for ammonia detection is shown in Figure 3-1.

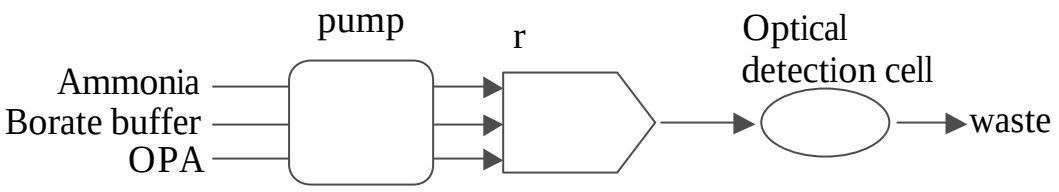

Figure 3-1 flow system used for ammonia detection by fluorimetry.

3.3 Cartridge elements

The experimental process starts with the fabrication and characterisation of the microfluidic elements required. Then these components are connected and the chemical parameters for the analysis are optimised.

3.3.1 Mixer

The control of the mixing of different fluids is an essential function in chemical analysis. In microfluidics the mixing of two fluids is more difficult than in a macroscopic situation, because the nature of the flow is laminar and the principal phenomenon enabling to mix two fluids is diffusion. Moreover at a microscopic scale it is very difficult to introduce turbulences to improve the mixer efficacy, and, to have a good mixing, it is necessary to maximise the surface contact between the liquids.

Mixers with different geometrical characteristics were fabricated in order to understand the role of each parameter. All the mixers are constituted by a channel with a rectangular section, 180 µm depth and with width between 150 µm and 500 µm and the length between 15 cm and 30 cm. A further parameter investigated is tortuousness of the channel introducing turns with different curvature radii.

Experiments to evaluate the mixing efficiency for different configurations have been conducted using mixers with two inlet ports, in order to introduce an acid solution of bromothymol blue sodium salt (Sigma-Aldric) and NaOH. The colour of the bromothymol solution depends on the pH of the solution, in the pH range 6.0-7.6 it changes from yellow to blue.

When the bromothymol solution enters in contact with the NaOH inside the mixer, the pH of the resulting solution changes and consequently a change in colour, from yellow to blue, is produced. Observing the uniformity of the colour in the channel it is possible to evaluate the length necessary to have good mixing.

Experimental results denote an important improvement of the efficiency of mixers with a high tortuousness, the smaller is the curvature radius of the turns the better is the mixing. A further parameter that affects the mixing is the flow rate, the lower is the speed of the fluid in the channel, and the shorter is the length of the channel necessary for the mixing.

It is possible to describe the characteristics that determine the efficiency in a mixer by defining the contact time. This parameter defines the time necessary for two fluids in contact in order to have good mixing. It is possible to influence the contact time with the width of the channel (narrow channels have a shorter contact time). A further parameter that reduces the contact time is tortuousness. In Figure 3-2 is shown a mixer during the tests with bromotymol and NaOH.

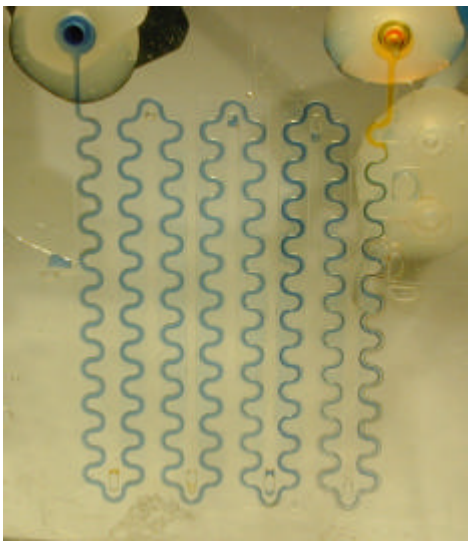

Figure 3-2 picture of a channel used as a mixer during a mixing tests

3.3.2 Optical detection cell

The design chosen for the optical cell is very simple and is constituted by a circular cavity with an inlet and an outlet ports (Figure 3-3). The dimensions of the cell are a diameter of 5 mm and a depth of 180 µm.

Figure 3-3 picture of a plastic optical detection cell

3.4 Material selection and characterisation

In order to select the most appropriate polymeric material to fabricate the final cartridge several characteristics are considered: optical characteristics and ease use of the polymers. Optical characterisations are performed on different polymers, in particular transmission spectra and fluorescent

emission are measured. The material chosen for the fabrication of the cartridge, as well as for the optical cell, is Epon 825. The cartridge is then closed by gluing a lid. The principal tests conducted are fluorescence spectra, with 370 nm excitation wavelength, and optical transmission spectra for Epon 825 and for different polymers in order to evaluate the best candidate for the fabrication of the lid.

In Figure 3-4 are shown the transmission spectra of the different polymers characterised. The first evidence is that polycarbonate, PMMA and Epon 825 do not have the good transmission property necessary at the excitation wavelength used.

Aclar 33C, Topas 8007 (transparent polymers used in packaging for pharmaceutical applications, with characteristics similar to the Teflon), and PMMA without UV stabiliser show good transmission for wavelengths from 300 nm to 600 nm. In particular the last one shows the best transmission characteristics as well as good performances in UV glue assembling process..

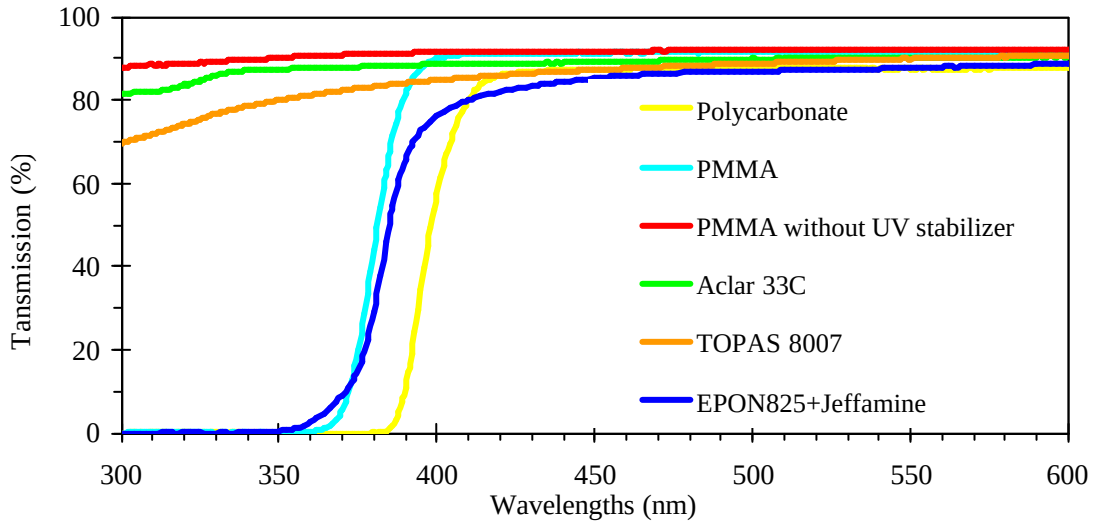

Figure 3-4 transmission spectra of different polymers (polycarbonate, PMMAs, EPON825+Jeffamine, Aclar 33C, TOPAS8007)

For the same polymers also fluorescence at 370 nm excitation is measured (Figure 3-5), polycarbonate is the only one that shows a strong fluorescence. For PMMA without UV stabiliser the intensity of fluorescence is very low, which confirms this polymer as the best candidate for the fabrication of the optical cell and the final cartridge.

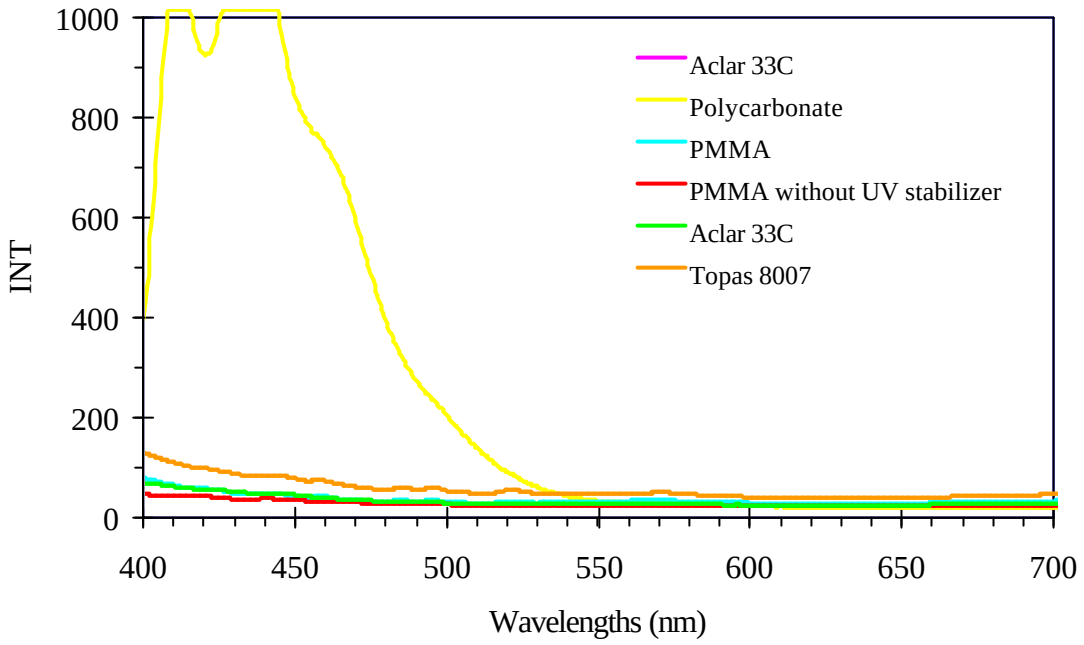

Figure 3-5 fluorescence spectra of different polymers: polycarbonate, PMMAs, Aclar 33C and TOPAS 8007 (excitation 370 nm)

For Epon 825 the situation is different, and a rather strong fluorescence is measured at a wavelength of 370 nm. In spite of this it continues to be the most convenient material to use for the mould-casting fabrication technique. Then it is necessary to find a way to eliminate its fluorescence.

The solution found to solve this problem is the addition of a black dye based on carbon powder. This reduces enormously the fluorescence of the Epon 825 without changing the mechanical characteristics of the polymer (Figure 3-6).

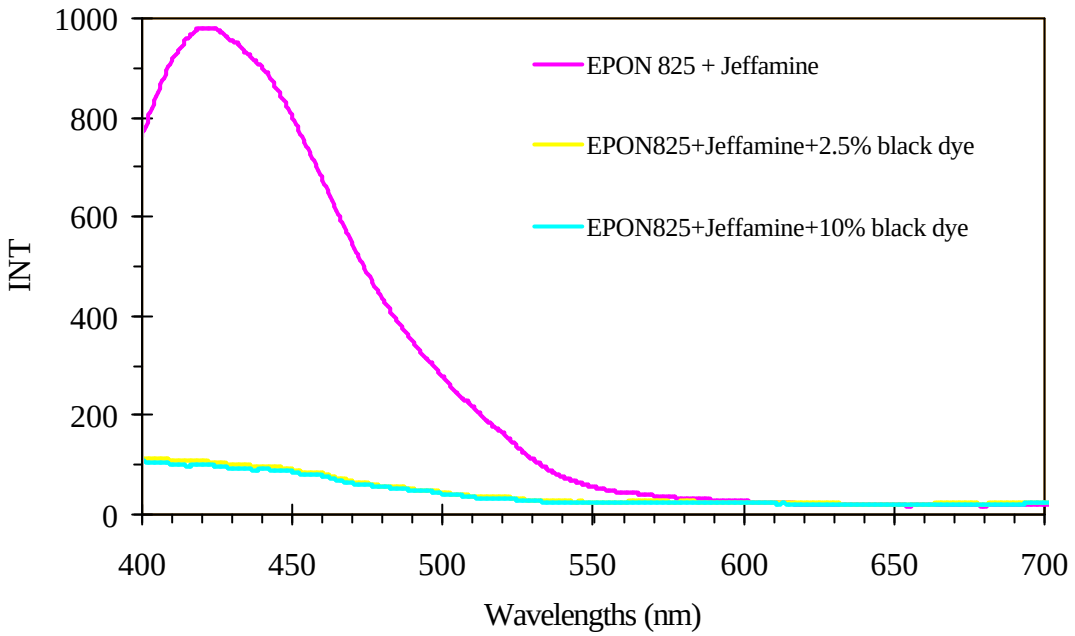

Figure 3-6 fluorescence spectra of EPON825+Jeffamine with and without black dye (excitation 370 nm)

3.5 Optical setup

The bench design is based on a one-beam fluorometer configuration (Figure 3-7). It simply consists of a light source, a dichroic mirror, excitation and emission filters, 3 collimating lenses and a photodetector. Because the dichroic mirror shows a non ideal behaviour, the use of excitation and emission filters is necessary. The former is an interference filter with a central wavelength of 470 nm. It is placed in the excitation path just prior to the dichroic mirror in order to select the excitation wavelength from the blue LED. The latter filter is a long pass filter with a cut-off wavelength at 500 nm, in order to select more specifically the emission wavelength and to remove traces of excitation light. This filter is placed after the dichroic mirror.

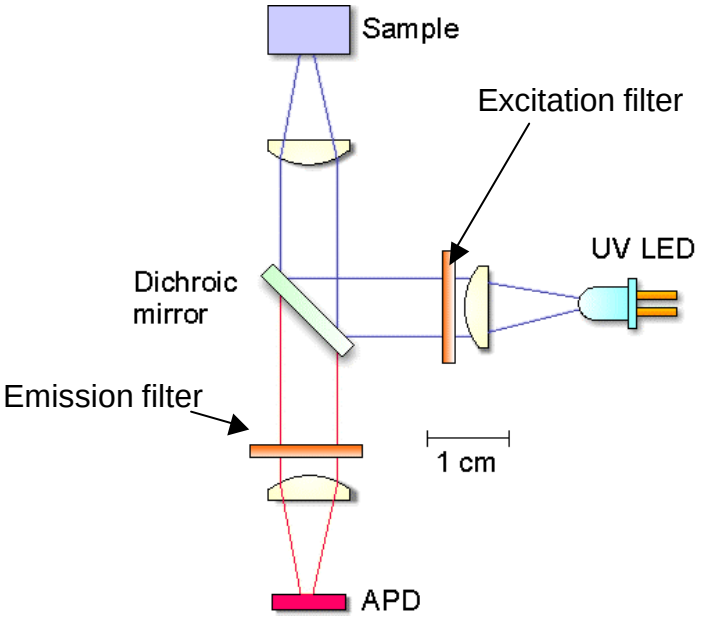

Figure 3-7 schematic view of the one beam fluorometer

This first bench configuration is optimised using fluorescein in aqueous solution at pH 9, detecting down to a concentration of 300 nM. Afterward the optical bench is adapted for detection of ammonia. The blue LED is replaced with a UV emitter (Roithner Lasertechnik, Austria) with an output at 370 nm, and the emission filter is set at 470 nm.

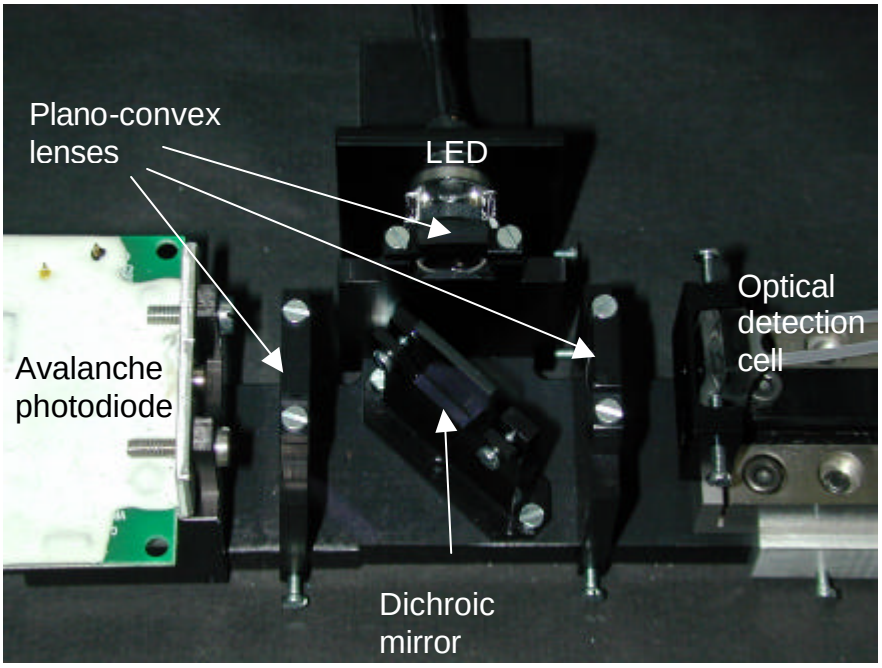

Figure 3-8 picture of the optical bench used with the cartridge for measurement of ammonia

3.6 Ammonia measurements

In aqueous solution of ammonia there is an equilibrium between NH_3 and NH^+_4:

$NH_3 + H_2O \Leftrightarrow NH^+_4 + OH^-$

and the proportion between NH_3 and NH^+_4 depends on the pH of the solution. OPA reacts only with NH_3, and the conversion of NH^+_4 to NH_3 in order to maximise the reaction, for this reason it is necessary control the pH of the solution. In the reaction a borate buffer is used in order to control the pH.

3.6.1 Modular approach

In order to optimise these chemical parameters, the measurements are performed with the microfluidic elements connected by plastic tubes, before dealing with the monolithic approach for the cartridge.

The experimental conditions for detection of ammonia are optimised by varying the concentration of OPA and thioglycolic acid, as well as the pH. The pH dependence of the NH_3 fluorescent signal is determined, with a maximum peak intensity around 9.6 (Figure 3-10). The influences of the concentration of thioglycolic acid and OPA are also investigated and are shown in Figure 3-11 and Figure 3-12. The fluorescence intensity reached a saturation level at approximately 30 mM in each case.

3.6.2 Monolithic approach results

After measurements performed with single microfluidic elements, in order to determine the best condition for ammonia detection, the mixer and the

optical cell are combined in a monolithic cartridge (Figure 3-9). The influences of the chemical parameters are again investigated in this new configuration. All experiments are performed at room temperature. Concerning the pH, OPA and acid thioglycolic concentration the same results as for the modular approach are found. These results are shown in Figure 3-10 for the influence of the pH, Figure 3-11 and Figure 3-12 concerning the thioglycolic acid and OPA concentrations. The flow rate is also investigated, and a maximum of the detection for ammonia is found for 108 µL/min.

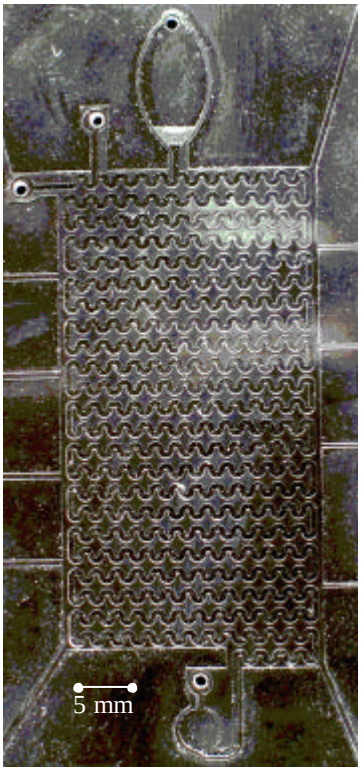

Figure 3-9 the final cartridge used for ammonia measurement

After optimisation of the ratio of the various chemical reactants, the monolithic cartridge is used to perform the measurements of ammonia with the parameters found for OPA and thioglycolic acid; ammonia detection

could be performed over three orders of magnitude with a detection limit of 10 µM (Figure 3-13).

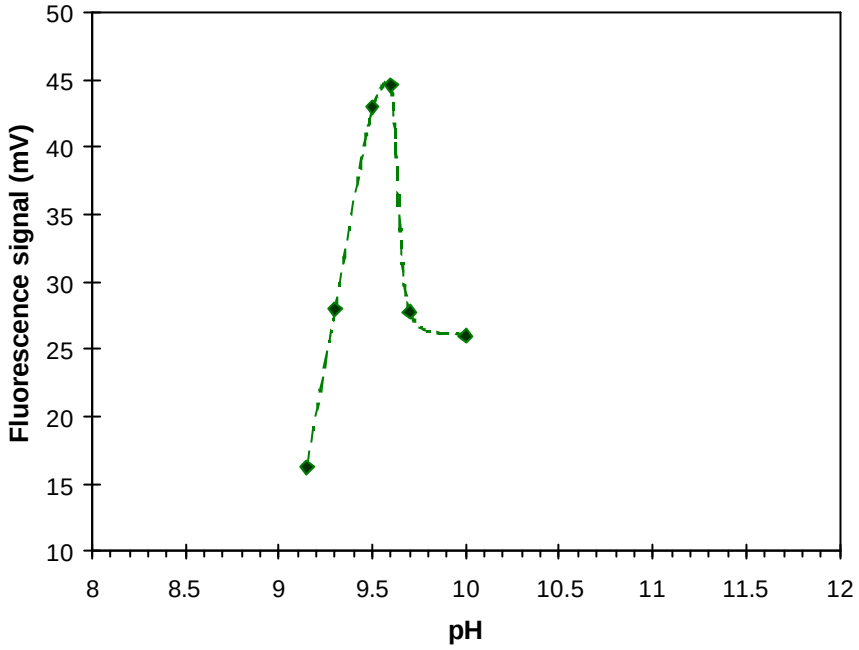

Figure 3-10 pH dependence of the NH_3 fluorescence signal – borate buffer at different pH, 10 mM NH_4^+, 30 mM OPA, 15 mM thioglycolic acid and flow rate 108 µL/min.

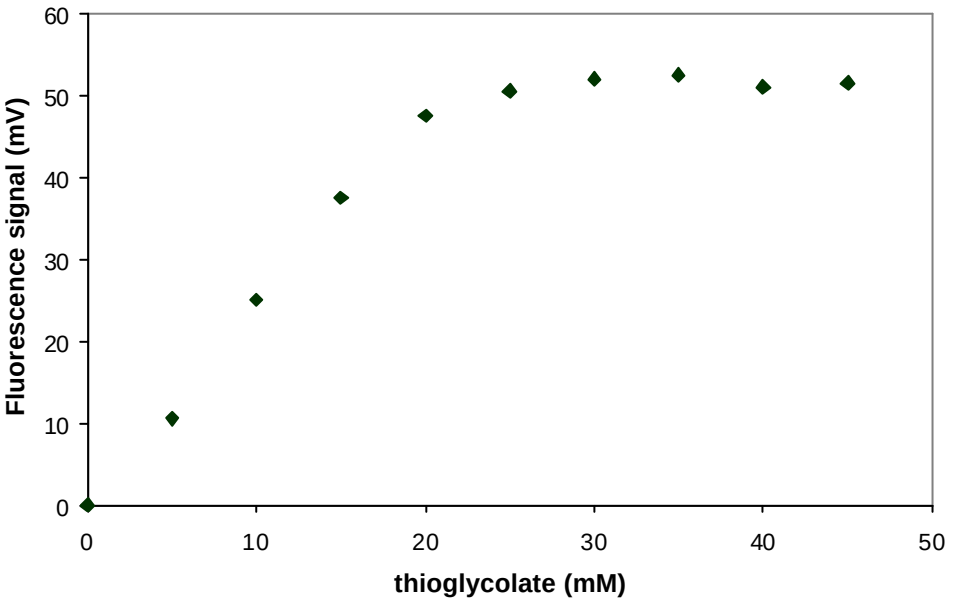

Figure 3-11 dependence of the NH_3 fluorescence versus thioglycolic acid concentration – 5 mM NH_4^+, 30 mM OPA, borate buffer pH 9.6 and flow rate 108 µL/min.

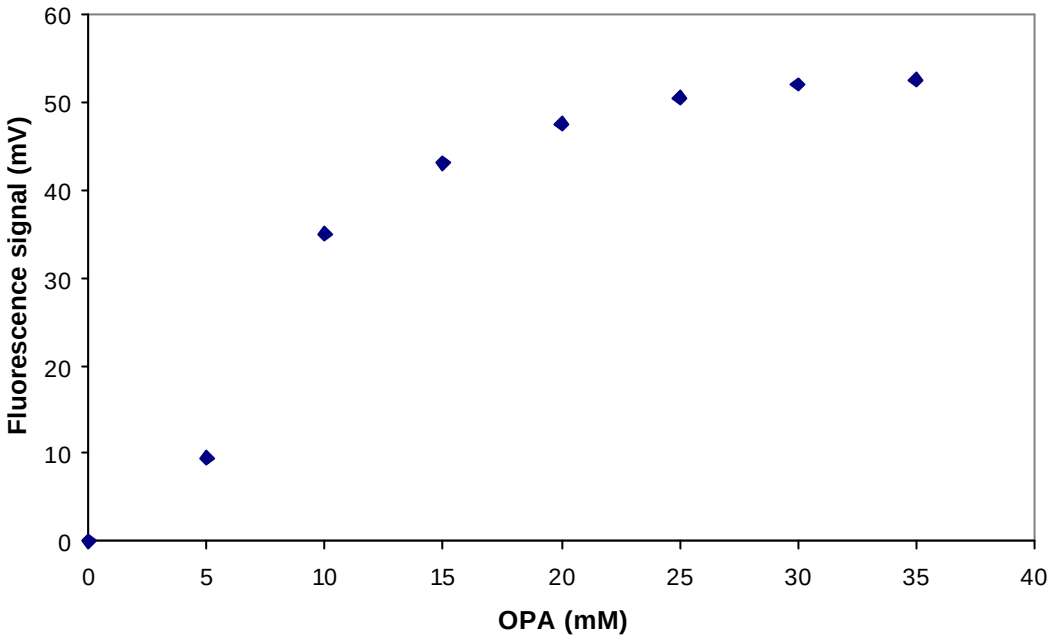

Figure 3-12 dependence of the NH_3 fluorescence signal on the OPA concentration – 5 mM NH_4^+, 30 mM thioglycolate, borate buffer pH 9.6 and flow rate 108 µL/min.

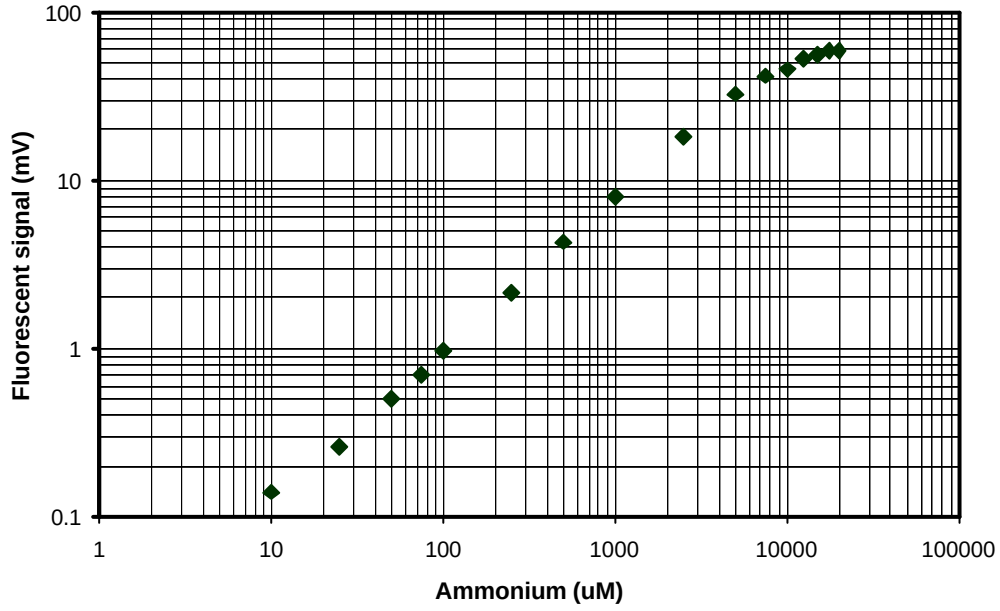

Figure 3-13 ammonium calibration curve – 30 mM OPA, 30 mM thioglycolic acid in borate buffer, pH: 9.6, flow rate 108 µL/min. Detection limit 10 µM

3.7 Conclusions

This chapter was focused on the fabrication of a cartridge for the detection of ammonia in aqueous solution.

For the realisation a modular approach has been followed, that means at first the chemical steps were analysed to identify the microfluidic elements necessary to be integrated in the final cartridge. Then every single component was realised and tested individually in order to find the best characteristics required for each one by the chemical assay. Finally all the single elements were integrated in a monolithic module. A first topic was the choice of the materials used for the realisation of the cartridge. As the detection of ammonia is by fluorescence, the optical characteristics of the polymers involved in the fabrication are of fundamental importance.

A further important result is the utility and the reliability of the modular approach. Analysis of a single microfluidic element means isolate this one from the whole system with a consequent reduction of the parameters to investigate in order to optimize the element. Once the components are optimised they can be integrated in a more complex system with the other elements.

4 Realisation of a Stop Flow Valve

4.1 Introduction

A microfluidic device consists of different elements like a sample injection or dosing part, a microreactor, a micromixer and a detection chamber. Among these components several elements to manage the fluid inside the cartridge are required. A crucial role is played by microvalves to gate the flow between the elements. In general two types of valves can be identified: passives valves and actives valves. The fundamental difference between them is the presence of an actuator for active valves, oppositely, for passive valves, no external actuation device is necessary.

The advantage of passive valves is that they reduce the number of elements necessary to be integrated in the final device, less electronics, no power supply and a less complicated technology to realise the cartridge.

Within passive valves two principal groups can be identified. The first set comprises all valves with a mobile part, based on a membrane or a circular mass suspended by two or four beams anchored on the device body [30], [31], [32], or a moving part inside of the microfluidic channel creating a piston based device [33]. A second category of passive valves can be realized by modifying locally the surface properties of a channel from hydrophilic to hydrophobic [34], [35]; or by creating an abrupt expansion of the channel cross-section [36], [37]. The latter approach is preferable if solvents and mixtures thereof are to be controlled. In both cases the liquid is prevented from entering the modified zone by capillary forces. The valve can be defeated when the liquid pressure at the meniscus is sufficiently large to

offset this “capillary barrier”. The model of the passive valve, developed in the frame of the project CREAM, presented in this chapter, belongs to this last category. The fabrication involves the use of micromachining technologies.

4.2 Model and designs

4.2.1 Interfacial energy

The behaviour of molecules situated at the interface between liquid and gas is different from that of molecules in the bulk that are surrounded by similar molecules and therefore in a totally isotropic environment. These symmetry properties are totally lost in the interfacial region where molecules interact both with similar molecules in the bulk region and molecules of gas phase. A such system can be described in term of energy changes in the liquid-solid-gas interface system. The total interfacial energy in a channel is described by

eq. 7 $$U = A_{sl}g_{sl} + A_{sa}g_{sa} + A_{la}g_{la}$$

where A_{sl}, A_{sa}, A_{la} are solid-liquid, solid-air and liquid-air interface areas, and γ_{sl}, γ_{sa}, γ_{la} are the corresponding surface energies per unit area. The surface energy is related to the equilibrium contact angle θ_c by the Young’s equation

eq. 8 $$g_{sa} = g_{sl} + g_{la}\cos q_c$$

Introducing this equation in the expression of the total energy gives

eq. 9 $U = (A_{sl} + A_{sa})g_{sa} - A_{sl}g_{la}\cos q_c + A_{la}g_{la} = U_o - A_{sl}g_{la}\cos q_c + A_{la}g_{la}$

where U_o is a constant as A_{sl} and A_{sa} are invariant.

The total energy is a function of the injected volume of liquid V_l: as V_l increases, the wetted area changes and the pressure is described by

eq. 10 $$P = -\frac{dU}{dV_l} = g_{la}\left(\cos q_c \frac{dA_{sl}}{dV_l} - \frac{dA_{la}}{dV_l}\right)$$

In an uniform and hydrophilic channel, i.e. $\theta_c = 90^o$, $\gamma_{sa} > \gamma_{sl}$, A_{sl} increases linearly with penetration distance. Therefore the liquid is aspired and wets the entire channel surface with a positive and constant pressure P driving the flow. The pressure P can be made negative by changing the surface properties to achieve $\theta_c = 90^o$ or by manipulating the channel geometry.

By definition the pressure barrier is equal to the pressure difference in equilibrium state. Assuming incompressible fluids, it can be demonstrated, from the last equation, that the pressure needed to move a fluid across an abrupt capillary expansion simply takes the form

eq. 11 $$\Delta P = 2g_{la}\cos q_c\left(\frac{1}{r_1} - \frac{1}{r_2}\right)$$

where ΔP is the pressure drop across the dimensional change, $r_{1,2}$ the radii of the capillary, g_{la} is the surface tension and q_c the contact angle between the liquid and the capillary walls.

4.2.2 First designs

In order to induce a pressure barrier to stop the liquid in a channel it is necessary to create an abrupt variation of channel width, with an expansion or a constriction.

Channel expansion can be conceived in different ways, the most simple is by changing the in-plane dimensions [37] as represented in Figure 4-1. This is the first design realised and tested in order to investigate if it could accomplish the functionality required in the development of the final cartridge.

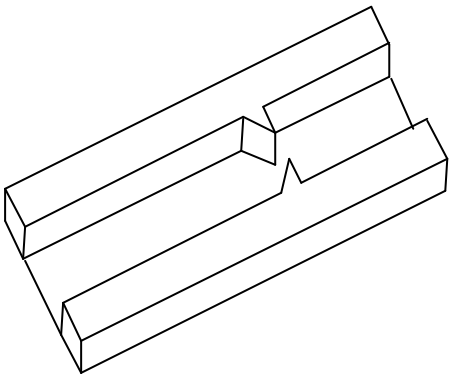

Figure 4-1 first design for a passive valve

To realize this design only one photolithography and a DRIE step is necessary. The entire fabrication process consists in a thermal oxidation of the wafer, photolithography, a wet etch (BHF) to open the silicon oxide and a DRIE. Finally the wafer is oxidized to make the channel surfaces hydrophilic, diced and the singles chips are closed with a pyrex lid by anodic bonding.

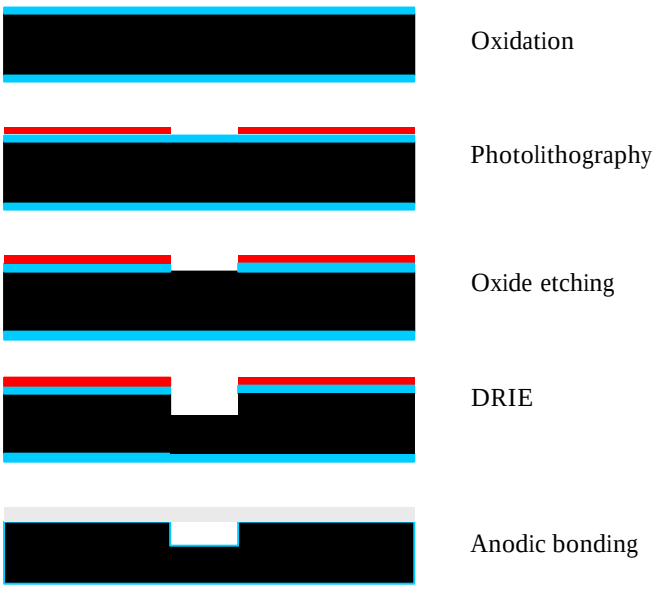

Figure 4-2 fabrication process for the fist design

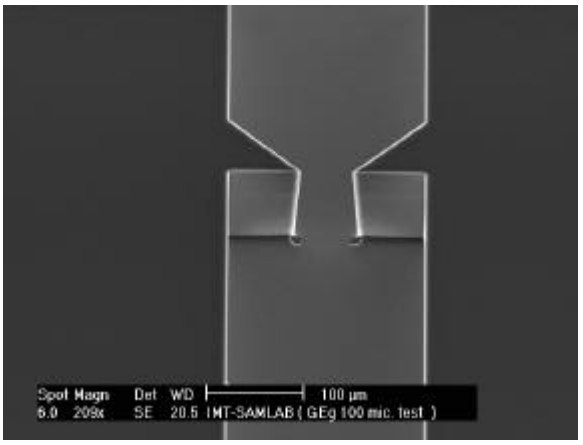

Figure 4-3 scanning electron microscopy image of a 2-D stop flow valve

Several channels, with different widths, are fabricated with this design. In order to test the functionality, water is introduced in the channel, and initially the liquid stops at the valve. However a formation of water film is observed on the walls of the valve and on the portion of the channel after the valve. Afterwards the bottom and the pyrex lid are wetted, and consequently all the channel is filled by the water defeating the valve.

Repeating the same test with a lower pressure of the water introduced in the channel the results are exactly the same.

The most likely the problem with this first design is that only a planar dimensional expansion is not enough to create the pressure barrier necessary to stop the flow.

4.2.3 Second design

In the second design of the stop flow valve a three-dimensional approach is considered.

The best solution to this purpose has been found in the following way. All the channels forming the microfluidic system are etched on top of the silicon wafer. For the valve, the channel is interrupted, and a wide and short channel is etched (expansion chamber) on the wafers' backside placed at channels' interruption, finally two narrow holes are etched through the whole wafer.

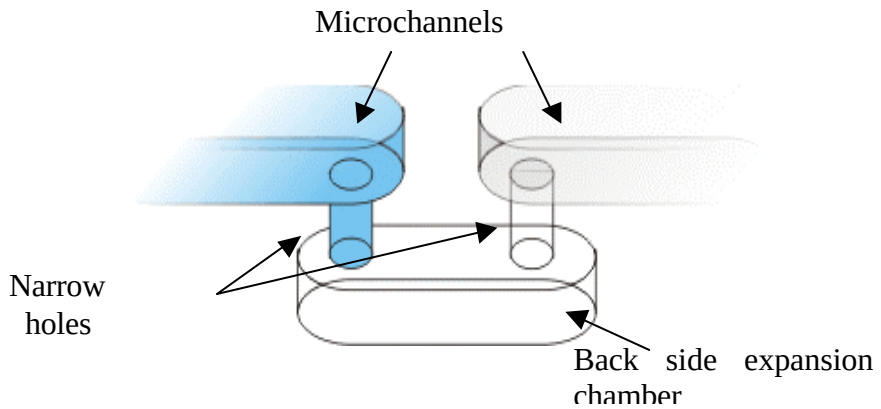

Figure 4-4 schematic drawing of two stop flow valves placed in series. The perpendicular interconnection channels expand into the larger section of the expansion chamber. Because of the symmetry of the design the stop flow valve can be used in either direction

A schematic view is represented in Figure 4-4. The liquid introduced in the microfluidic system fills the channels. At the valve the narrow hole is filled

by capillarity, and the barrier of pressure is created between the hole and the expansion chamber on back side.

4.3 Fabrication Process

The fabrication process of the valve is presented in Figure 4-5. The final device consists of three parts, the microfluidic system realised in silicon which is structured on both sides, and two cover plates in pyrex. The microfluidic system is realised on a double polished silicon wafer 390 µm thick, on the top side is patterned the channel network, and on the back side the expansion chambers for the valves.

The fabrication process starts with the oxidation of the silicon wafer, to form oxide thickness of about 1.5 µm. A first photolithography is performed using the positive di-azo resist AZ1518 (Clariant, Muttenz, Switzerland), a layer of about 1.8 µm is spin coated onto the wafer after which a pre-bake step at 100 ^{o}C on a hotplate is done in order to remove solvents from the resist layer. The wafer is exposed to UV-light using a mask aligner (MA-6 Karl-Süss), the photoresist is developed and the wafer is post-baked in an oven to further strengthen its stability.

The patterned photoresist is then used as an etching mask for a wet etch in BHF to open the oxide over the channels area, then the photoresist is stripped and a second photolithography is performed to create the valve holes, this time with the positive resist AZ4562, that allows thicker spin coated layers, necessary to create a mask for a DRIE.

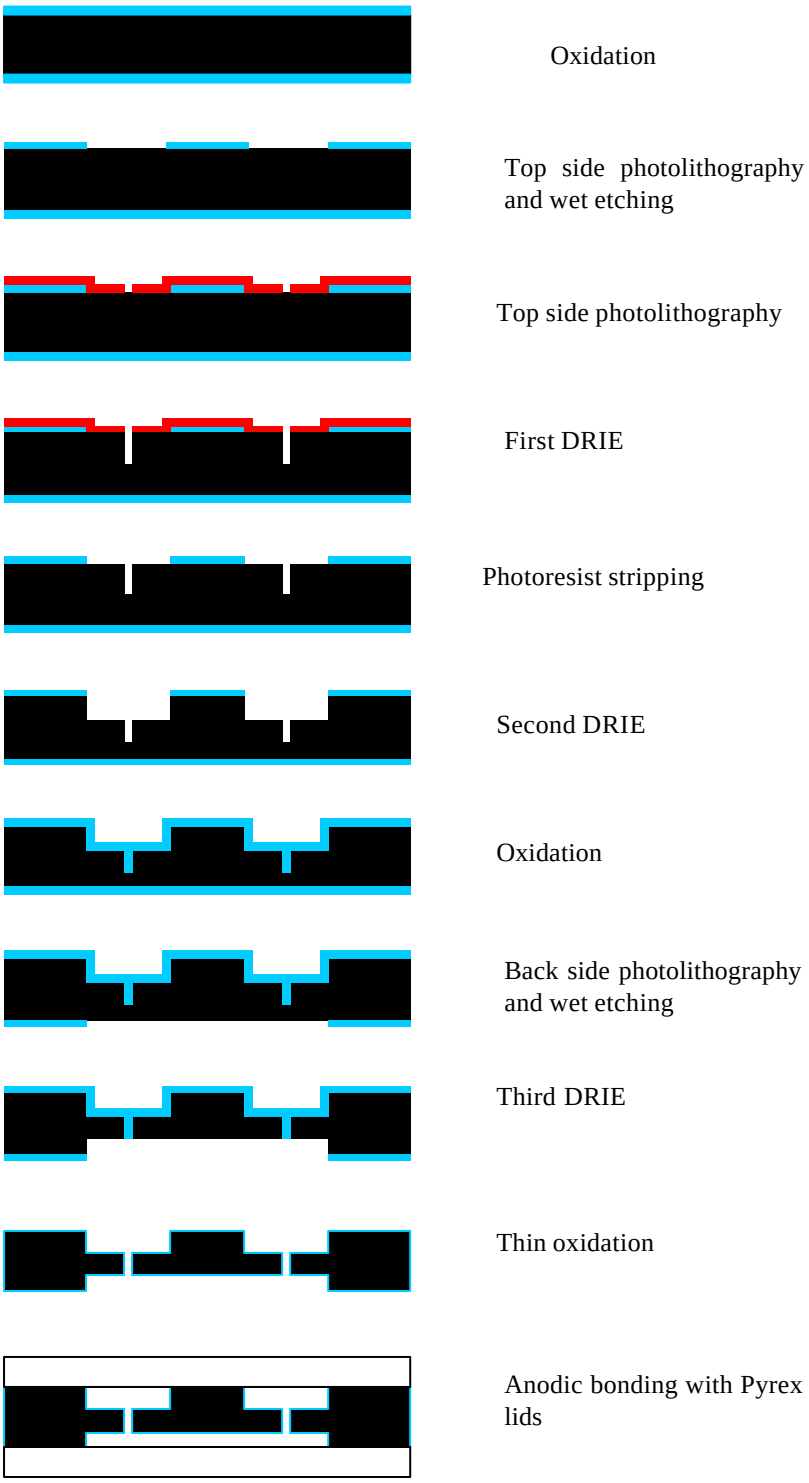

Figure 4-5 schematic process sequence for fabrication of the microvalves

A first DRIE is made, the depth of etching is about 200 µm, after photoresist stripping a second DRIE is done with a depth of about 100 µm. At this point all the oxide is etched, the wafer cleaned and again oxidised; now the wafer is ready for back side patterning with a third photolithography, again with AZ1518 resist, an oxide wet etch and the last DRIE. This last etch is performed till the holes are open (see Figure 4-6); after that the wafer is again cleaned in order to eliminate all residues of photoresist and a thin oxidation is performed to make the channels hydrophilic.

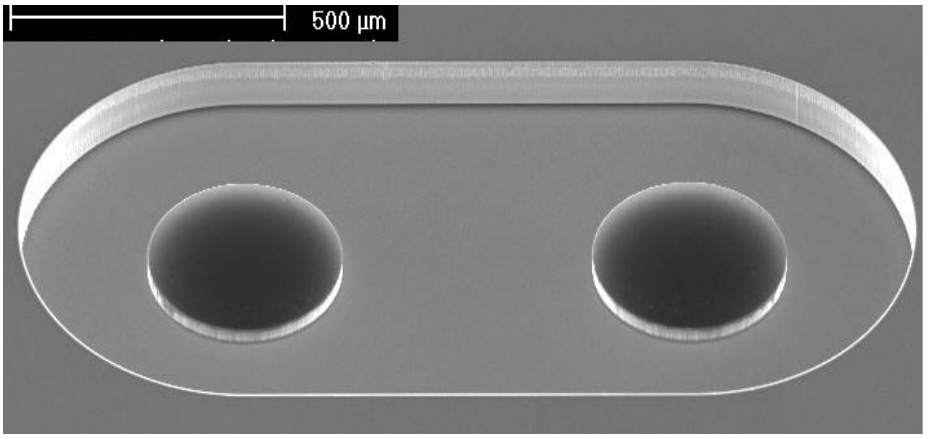

Figure 4-6 close-up view of two stop flow valves (backside view) during manufacture. The etch depth of the expansion chamber is selected to partly release the valves. (Scanning Electron Microscopy image)

4.4 Tests and Characterisation

Before integrating the valves in a complex microfluidic device, a system for testing their functionality is realised. The experimental system is designed for

a sequential test of a set of valves with different diameters and different dimensions of the expansion chamber.

In order to show that the valve principle works, i.e. to see if the liquid is stopped at the expansion, the valve, more precisely the expansion chamber, is observed with a fluorescence microscope while a solution of fluorescein in water is introduced in the channel using a weak pressure (Figure 4-7). It is possible to observe that the fluorescent liquid fills the vertical capillary, and it is stopped at the expansion. Increasing the pressure, the valve breaks down and the whole expansion chamber is filled with the fluorescent solution. Next step is to evaluate experimentally the pressure necessary to defeat the valve and compare the results with the calculated values.

a) 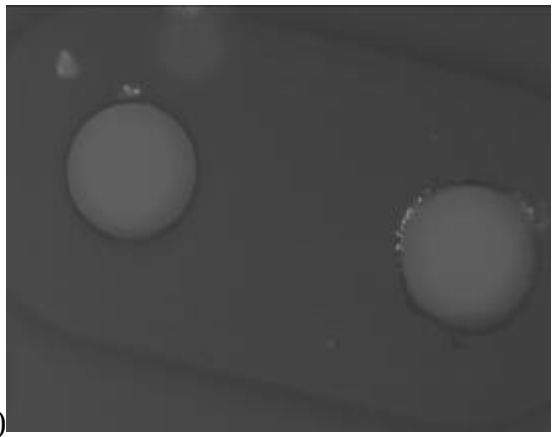 b) 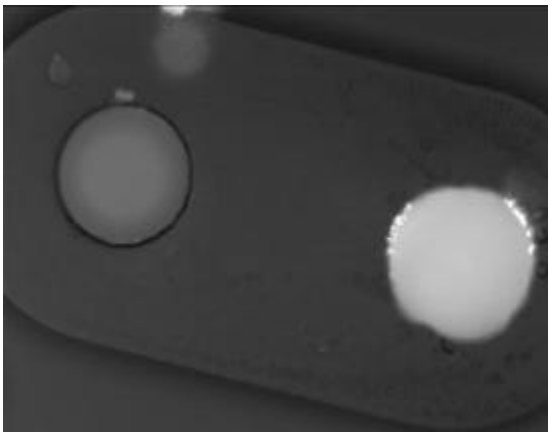

Figure 4-7 a valve during functionality tests (back side). View of the expansion chamber at the fluorescence microscope a) before introducing the fluorescein solution, b) with the solution stopped at the capillary

A cylindrical container is connected to the channel with the valves, and by introducing water in the container, the channel is filled by capillarity. The water is stopped by the valve, the height of the water column in the container is a measure of the pressure applied. By varying the water level in

the container it is possible to change the pressure applied to the valve. By Measuring the height of the column when the valve breaks down it is possible to have the experimental evaluation of the pressure that the valve can support (Figure 4-8).

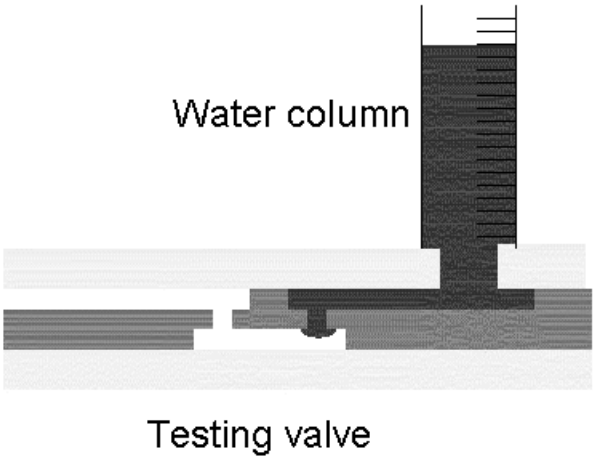

Figure 4-8 outline of the experimental setup used to test the valves

The theoretical pressure that a valve can support is calculated applying eq. 11 using for r_1 the internal valve radius and for r_2 the expansion chamber width, the value of the surface tension of water (s) is 0.073 N/m [35], for the contact angle a mean value of 35^o has been taken.

Generally the measured values of the maximum admissible pressure is fairly close to the calculated values; especially for the valve with larger radius (200-50 μm). The valves with smaller radius (<50 μm) can be defeated with lower pressures than the theoretically inferred. A possible explanation could be the etched surface roughness might cause effects that became important at small diameters, although these effects are negligible with bigger diameters. Valves have been also tested with isopropyl alcohol and the maximum admissible pressure results approximately half of the value obtained with water (Table

2). This is due to a lower surface tension and a smaller contact angle between silicon oxide and isopropyl alcohol.

r_1 (±2 µm)	r_2 (±2 µm)	Pressure (millibar) Experim.	Theor.
187	250	1.4±0.5	1.6
95	145	4.3±0.5	4.3
65	145	10±2	10.2
58	200	13±2	14.5
31	250	27±5	33.8
29	145	15±5	32.3

Table 1 maximum admissible valve pressures with water, calculated using q_c : 35° and s: 0.073 N/m (10 replicates)

r_1 (±2 µm)	r_2 (±2 µm)	Pressure Experim. (millibar)
95	145	2.0±0.5
65	145	4±2
58	200	6±2
31	250	15±5

Table 2 maximum admissible valve pressures with isopropyl alcohol

4.5 Conclusions

In this chapter the realisation of a passive stop flow valve is described. The principle of function of the valve is based on capillarity effect, the valve has

thus the advantage to work without any actuation systems, and with aqueous solution and isopropyl alcohol.

The valve can become the basic element for the realisation of more complex microfluidic components for fluid handling, some examples are described in chapter 5.

5 Stop flow valve applications

5.1 Introduction

As seen in chapter 3, it is possible to realise a cartridge for chemical analysis by integration of different microfluidic elements. Each component is designed and optimised in order to accomplish a specific step in the process. In this chapter design consideration, realisation and tests are described for several microfluidics devices. All these systems exploit the principle of the stop flow valve described in chapter 4. Although the components are realised for the cartridge for the detection of β-lactams in milk, they could find applications in a wide range of microfluidic application in life science and chemistry.

5.2 Sample metering system

5.2.1 Introduction

Generally, in order to perform a chemical analysis, the first step is to collect the sample, i.e. some deciliters of milk at the farm. This sample is transported to the chemical laboratory, where a precise amount is metered, usually from a few microliters to several millilitres. Finally analysis starts with the required steps, as mixing with other chemical solution, filtration and so on. The step of metering of a precise amount of sample for the analysis is usually performed with the help of specific volumetric or gravimetric tools like micropipettes or high precision balances.

One of the advantages of realising a cartridge is that the analysis could be performed on site, eliminating the transport of the sample to the laboratory. Sample injection and dosing are important functions required in miniature chemical analysis systems. Sample must be first injected into the system, metered in a specific volume, and properly routed to the reaction chamber [50]. These functions can be accomplished, for example, using a series of valves that control the extent and flow of the sample. A sample metering system is a structure integrated in the cartridge performing this function.

5.2.2 Design and realisation

This section shows a metering system produced using the valves described in the previous chapter. The metering principle is represented schematically in Figure 5-1 and consists in an introduction port for the sample, a capillary and two valves, one of which acts as air vent.

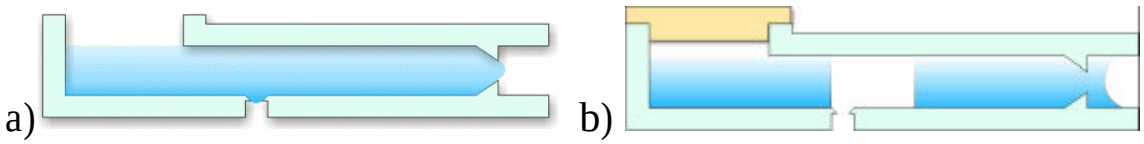

Figure 5-1 metering principle. a) the sample is introduced in a sample well. Liquid fills the capillary until the stop flow valve is reached. b) The sample well is then closed and air is injected through the air vent. The meniscus flows over the stop valve and a metered section enters the system

The final design of the sample metering system, shown in Figure 5-2, is fabricated using a 390 µm thick silicon wafer, the fabrication steps are the same described for the stop flow valve (Figure 4-5). The metering channel,

the reactor and the introduction port are etched during the second DRIE; the connections for the valves (expansion chambers) are etched on back-side of the wafer. Finally the chip is closed on the top and bottom by pyrex lids into which holes for fluidic connections are drilled by ultrasonic drilling.

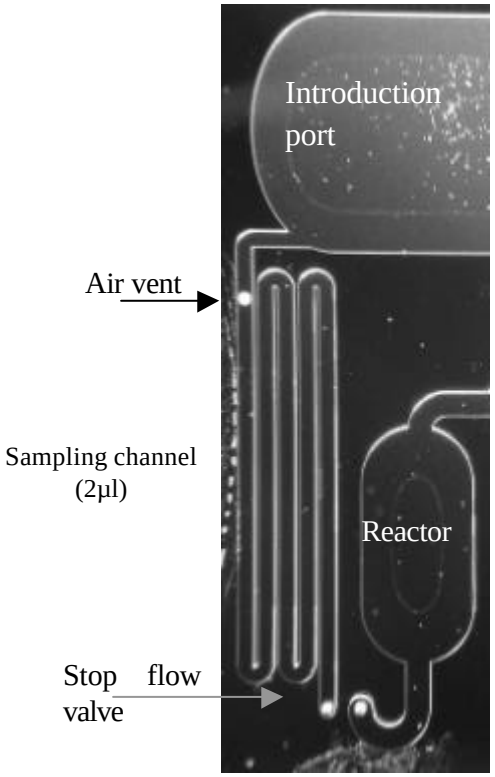

Figure 5-2 picture of the sample metering system. The metering channel is 5 cm long, 400 µm wide and the depth is 100 µm. The final volume of 2µl.

5.2.3 Functionality tests

For functionality tests, two models of metering systems are realised with different volumes, a first one is designed to meter a volume of 2 µl, and the second one 4 µl.

After the fabrication is completed the real dimensions of the devices are measured in order to evaluate the practical volume. These dimensions are the following: 416±2 µm wide, 165±1 µm deep, and 31.2±0.1 mm and 62.5±0.1 mm long for the 2 µl and 4 µl, respectively. These measures give exact volumes of 2.14±0.02 µl and 4.29±0.03 µl.

The precision and repeatability of both sample metering systems are characterized with water. Upon dispensing a drop of water in the sample port, the liquid penetrates into the metering channel by capillarity until it reaches the first stop flow valve. The introduction port is closed and air is injected through the air vent with a syringe to separate the sample in channel from the bulk. The sample is then pushed beyond the valve and collected in a tube connected with the device. Collected sample fractions are weight with a precision scale (Mettler Toledo AG245). The results are presented as histograms in Figure 5-3.

Considering that the precision of the experimental measurements is limited by the sensitivity of the scale which introduced an uncertainty of ±0.1 µl, the mean values calculated for 20 replicates result to be 2.15 µl and 4.30 µl with a standard deviation of 0.08 µl and 0.06 µl, respectively. These experimental results are quite similar to the target volumes calculated from the geometrical parameters of the devices.

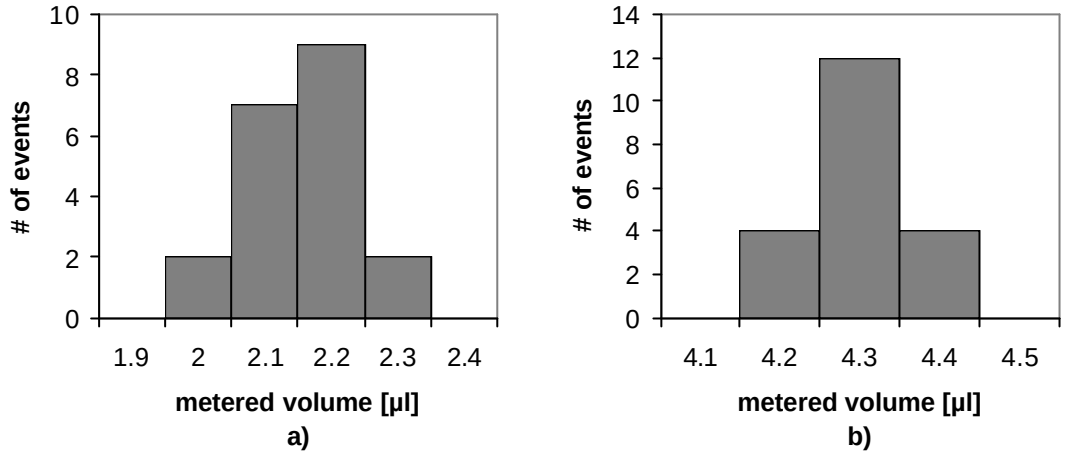

Figure 5-3 distribution of the sample volumes metered experimentally (20 replicates) with the sampling devices for 2 µl (a) and 4 µl (b).

The same devices were successfully used to meter a selection of organic solvents. These include acetone, methanol, γ-Butyrolactone (99%), acetonitrile (99.5%), dimethylsulfoxid (99.5%) and toluene (99.5%). The purpose of these last tests is to verify that the sample metering system functions not only with aqueous solution, but also with organic solvents with different polarities.

5.3 Micro Drier

5.3.1 Introduction

In this section an additional microfluidic element is described, the realisation of which is connected with the development of the cartridge for the project CREAM. The need of this element stems from the fact that MIPs work in a solution of almost pure acetonitrile (95%). The milk, after protein

precipitation, is an aqueous solution, therefore it is necessary to eliminate the water and substitute it with acetonitrile.

In order to dehydrate the sample solution different possibilities are considered, such as the use of desiccants, nanofiltration, pervaporation and evaporation. A further parameter to consider is the possibility of recuperate the solid part after dehydration in order to dissolve it in acetonitrile.

The desiccants such as molecular sieves, magnesium sulphate, calcium chloride, calcium sulphate and sodium sulphate are of common laboratory use for removing trace amount of water. As the proportion of water contained in a sample can reach up to 50 % of its volume, large amounts of desiccants are needed for dehydrating the sample. Furthermore these substances can interact with acetonitrile and these chemical compatibilities have to be considered.

Nanofiltration is a pressure driven membrane process with performance characteristics between reverse osmosis and ultrafiltration. Nanofiltration membranes have very good rejection rates of particles in the molecular range (5 nm to 50 nm) or, equivalently, a molecular weight greater than 1000 Daltons. The effective driving pressure in a nanofiltration system is the gauge hydraulic pressure minus the osmotic pressure differential. For optimum separation performance, about 14 Bar effective pressure is required and performance falls off markedly below 7 Bar. This pressure range precludes the integration of nanofiltration in a microfabricated device as a cartridge.

Pervaporation (permeation and evaporation) is a membrane process used industrially for the dehydration of organic solvents or the removal of organics from aqueous streams. Unlike other membrane processes, pervaporation requires a brief phase change from liquid to vapour to

separate the influent stream into two effluent streams, the permeate and concentrate. Transport of the permeate through the membrane is driven by a difference in pressure maintained across the membrane. A partial vacuum on one side of the membrane is used to draw the permeate through the membrane barrier to create a permeate vapour which is immediately condensed and removed, leaving an enriched concentrate solution. This partial pressure can be lowered by using a vacuum pump or by a flow of inert gas. Although membrane materials govern the pervaporation process and determine the separation factor, operational conditions do effect the permeation flux and selectivity. With the use of a temperature gradient of 50 °C and a 10 mBar vacuum, permeate fluxes in the range of 10 kg/m^2h can be reached. The dewatering of 100 µl of 50% solvent across a 1 cm^2 membrane would technically be possible in less than a minute. To successfully integrate this technique in the cartridge, operational conditions leading to a reasonable pervaporation time must be created in a very confined environment. A partial downstream pressure lower than the saturation pressure could be generated in the cartridge by means of a Venturi tube. A channel constriction would cause the velocity of an inert gas to increase and the pressure to fall in this section. A reasonable temperature gradient could also be produced by the adiabatic expansion of the same inert gas. Moreover, cooling of the permeate side would be preferable as the heating of the retentate side would degrade the β-lactam molecules. Yet, although membranes with high flux rates and high separation selectivity towards water have been reported, none are suitable for our purpose. In-house development of such membrane is out of scope.

As an alternative to pervaporation, the entire sample can be evaporated. Since the β-lactams are not volatile, the dried fraction can then be re-diluted in the proper solvent composition. This approach appeared to be the most promising for a cartridge application and was further considered. Taking into account that the species of interest would degrade with an increase of temperature, other variables must be optimised in order to improve the evaporation process.

5.3.2 Evaporation rate

Evaporation takes place because of a non-equilibrium state between the liquid and the gas phases. The internal pressure P_1 in a droplet delimited by a curved surface of radius r_1 is different from that of a surface with radius r_2. This is expressed by the general form of the Kelvin equation [51]

eq. 12 $$\ln \frac{P_1}{P_2} = \frac{2gV_M}{RT}\left(\frac{1}{r_1} + \frac{1}{r_2}\right)$$

where V_M is the molar volume of the species, ? is the surface tension and RT have the usual meanings. For the simple case of a flat surface ($r_2 = r_0 = \infty$ and $P_2 = P_o$) the above equation simplifies to:

eq. 13 $$\ln \frac{P_1}{P_o} \approx \left(\frac{P_1 - P_o}{P_o}\right) \approx \frac{2gV_M}{r_1 RT}$$

The following empirical expression relating the time t_d needed for a droplet of radius r to evaporate can be established:

eq. 14 $$t_d \approx k\, r^2$$

where k is an evaporation constant (4000 $\mathrm{sec/mm^2}$ for pure water, at room temperature, 50% humidity and at atmospheric pressure).

Assuming that a volume of 10 µl is to be evaporated in a space of time in the range of a minute, from eq. 14 it results that this volume needs to be converted in a set of 2400 spherical droplets. These droplets have a diameter of 200 µm and they evaporate simultaneously, a schematic view of the evaporating device is shown in Figure 5-4.

By dividing the total volume V_T in droplets of radius r over a droplet volume of V_d, the total number of droplets N_d is

eq. 15 $$N_d = \frac{V_T}{V_d} = \frac{V_T}{\frac{4}{3}pr^3}$$

Assuming that all droplets are generated instantaneously and distributed in a channel of length L_o:

eq. 16 $$N_d = \frac{L_o}{2r + w}$$

where w correspond to the distance separating the droplets. Equating eq. 15 and eq. 16 gives

eq. 17 $$\frac{L_o}{2r + w} = \frac{3V_T}{4pr^3}$$

Introducing eq. 14 in eq. 17 relates the evaporation time to the geometric parameters of the “evaporation” device:

eq. 18 $$t_d = \frac{3V_T(2r+w)}{4prL_o}k$$

Practical radii that can be generated in small channels range from 10 to 50µm. Setting the distance L_o within 50 to 500 mm and setting w at a fixed value of 10µm, surface and contour plots were produced to facilitate the “evaporator” design.

To enhance and control the evaporation rate, dry inert gas can be flushed over these “droplets”. In a similar manner as described above the same gas will lower the partial pressure at the evaporation side and enhance the formation of menisci.

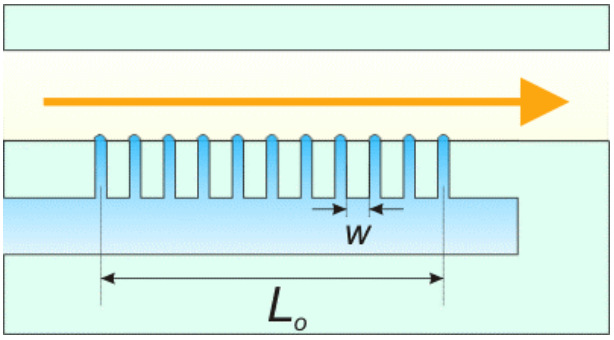

Figure 5-4 schematic view of the evaporating device

5.3.3 Designs and realisation

To realise the dryer it is necessary to find a way to create an interface between the liquid to evaporate and the air. The solution found is to use the principle of the valves described in chap. 4. The first design of the micro drier (Figure 5-5) is based on the first generation of valves, but, as already

mentioned in paragraph 4.2.2, this type of valve suffers from the formation of a film of water on the silicon structures. Despite of this, it is possible to observe the evaporation of the water; this confirmed that a device based on evaporation is feasible.

a)

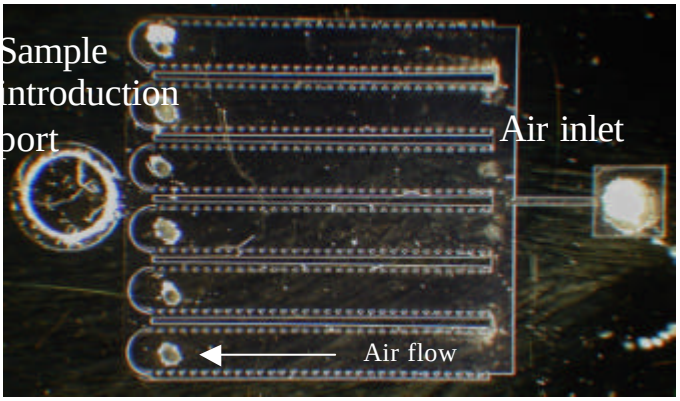

b)

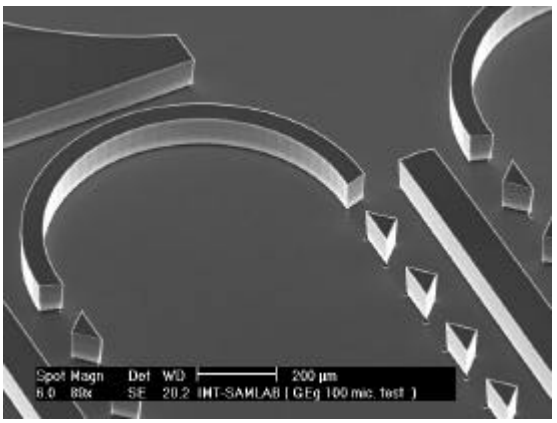

c)

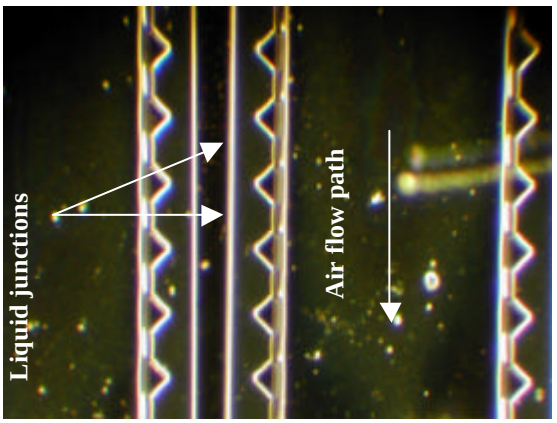

Figure 5-5 a) picture of the first design of the microdrier, b) SEM image of a detail, c) picture of the microdrier when filled with water.

With the realisation of the final design of the valve a new version of the microdrier is fabricated. It basically consists of a channel in which a set of vertical capillaries is realised, connecting to a chamber through which an air flow is passed (Figure 5-4). The microdrier is integrated with a sample metering system of 3 µl, and it is constructed in such a way that it is possible to rinse the metering channel after evaporation, then meter the required

solvent, flow this solvent through the evaporation channels in order to dissolve the solid deposited during evaporation, and finally extract the new solution from the device.

The realisation of the evaporator starts with a silicon wafer and the fabrication steps are exactly the same as that of the stop flow valve (description of the technology in Figure 4-5, paragraph 4.3).

5.3.4 Functionality tests

The device shown in Figure 5-6 is the result of the integration of a sample metering system with a microevaporator. Introducing the sample in the port, a volume of 3µl is metered from the sampling channel. Closing the sample port and applying a pressure at the air vent, the sample is transferred in to the evaporator channel, air flowing on the back side make the solvent evaporating. After evaporation it is possible to rinse the metering channel flowing water from the air vent to the waste, the special three channel valve, showed in Figure 5-8, acts as a switch. The valve connects three channels: the metering and the evaporating channels and the channel leading to the waste. The three holes of the valve (A, B and C) have different diameters, in order to support different pressures. When the waste channel is closed and a pressure is applied at the air vent, the liquid defeats the valve A and C getting inside the evaporation channel. Moreover if the waste is open and the valve is dry, applying a pressure the valve A is defeated, but the fluid flows through the hole B to the waste. The evaporating channel is 56 mm long and 300 µm large, it contains 371 holes with a diameter of 40 µm. The

whole chip measures 30x20 mm. On the back-side of the device there is the evaporating chamber where dry air is flowed.

a)

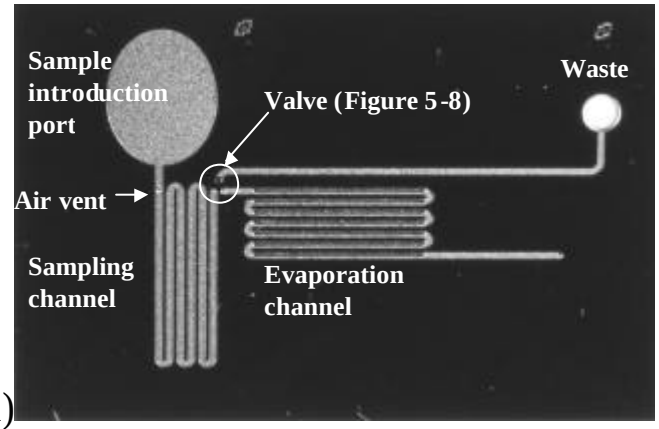

b)

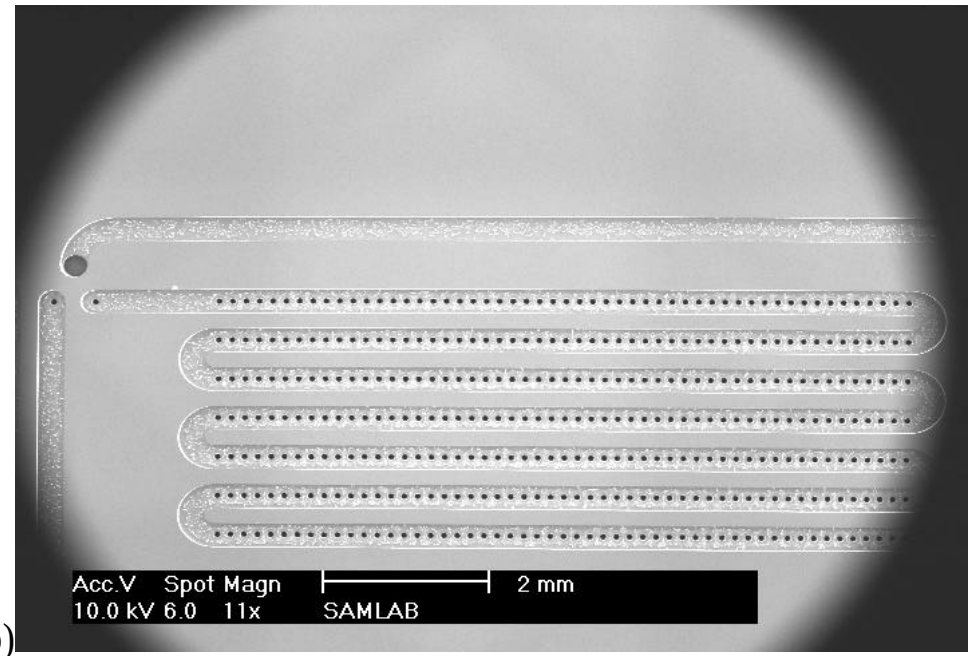

Figure 5-6 evaporating device, top side view (a).b) details of the evaporating channel. The channel is filled with liquid and the holes are the capillaries connecting top side with back side to generate droplets to evaporate.

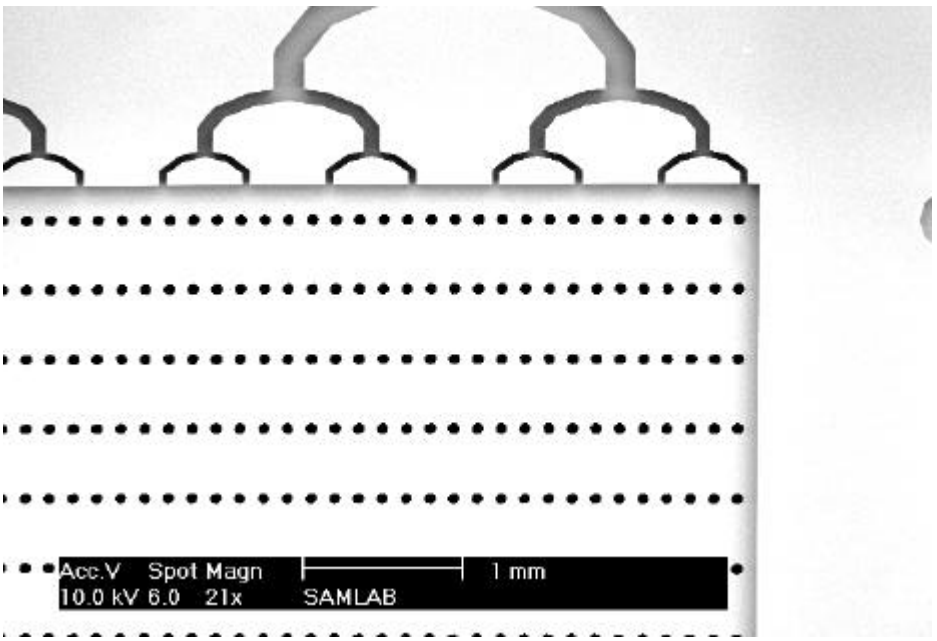

Figure 5-7 the evaporating chamber on the back side of the device.

a)

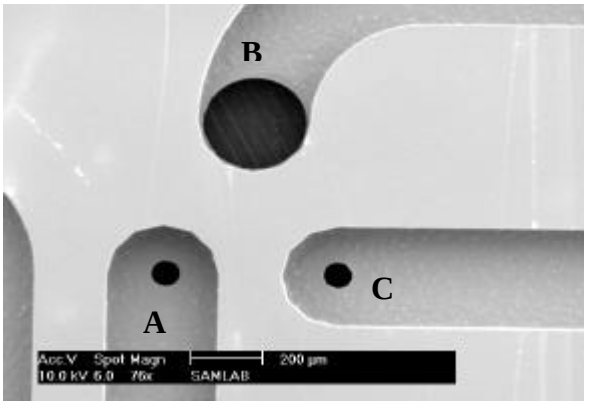

b)

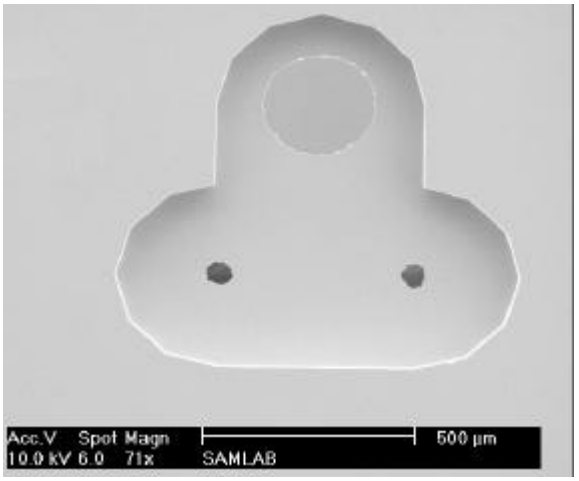

Figure 5-8 three channel connecting valve (switch),a) Top side and b) Back side (SEM image)

The efficiency of the evaporator is evaluated by performing an evaporation inside the device and evaluating the evaporation time of the solvent as a function of the air flow. The device is connected with a mass flow controller

(Bronkhorst Hi-Tec, F 110C) to control the air flow, tests are conducted at room temperature. The evaporator is filled with 3µl of isopropyl alcohol and contacted with a flow of dry air on the back side. Evaporation time is measured with different flow rates (Figure 5-9). Then a mixture of water and isopropyl alcohol in different ratios are also evaporated with a fixed air flow rate (Figure 5-10).

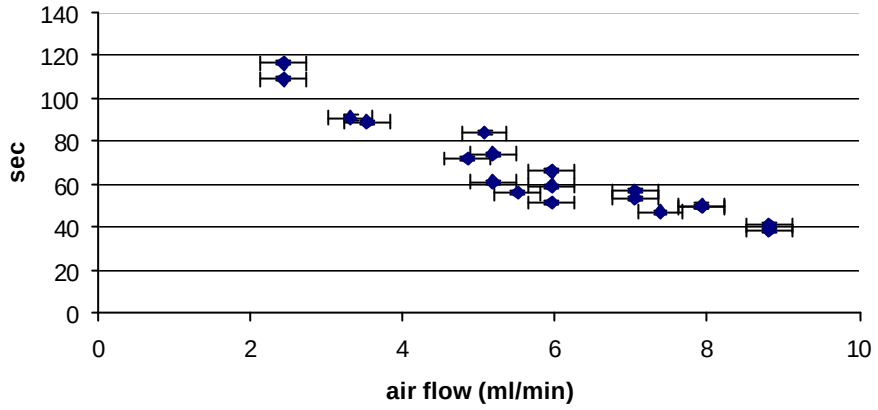

Figure 5-9 drying rate of 3 µl of isopropyl alcohol as a function of different air flow rates

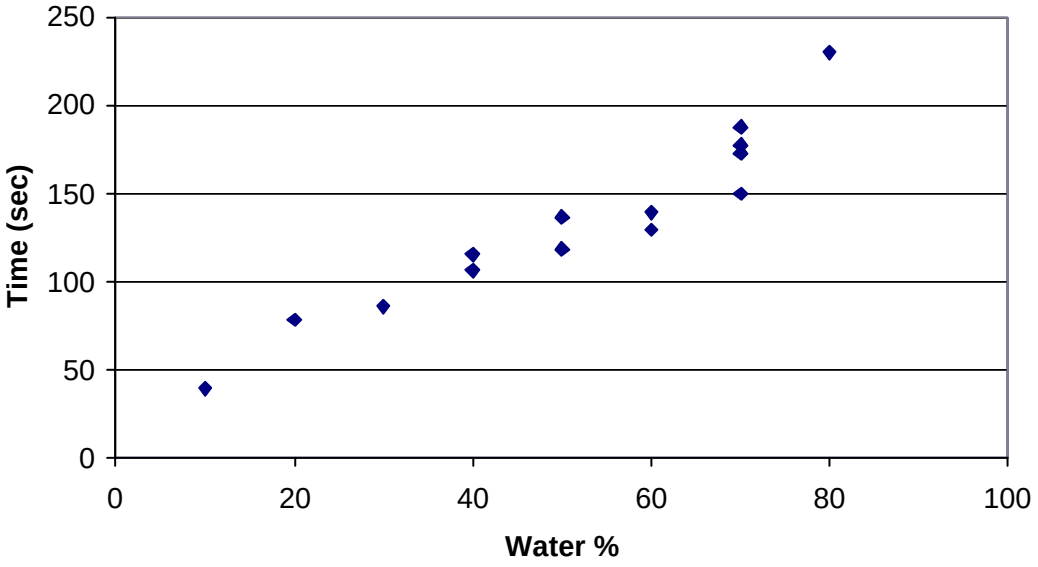

Figure 5-10 drying time of 3 µl of a mixture of isopropyl alcohol and water versus water percentage, maintaining a fixed air flow (9 ml/min).

Finally, the recovery rate of the solids that are deposited in the channel is evaluated. Tests are conducted with solutions of NaCl, and the method of detections used is conductometry.

A schematic view of the tests is shown in Figure 5-11. An aqueous solution of NaCl (0.5 M) is introduced in the sampling system integrated with the drier. The metered part of this solution (3 µl) is introduced in to the drier and all the water evaporated by the air flow. After evaporation, the sampling system is rinsed with water, and the rinsing water is directed to the waste. Then the evaporation channel is rinsed by flowing 5 ml of water. During this rinse the deposited salt dissolves and the solution is recovered outside the device and is added up with water till 20 ml (experimental solution). In parallel, a second solution is prepared from the stock solution (0.5 M) by taking 15 µL and adding water to 100 ml (reference solution). The two solutions, theoretically, have the same concentration of salt, therefore should have the same conductivity.

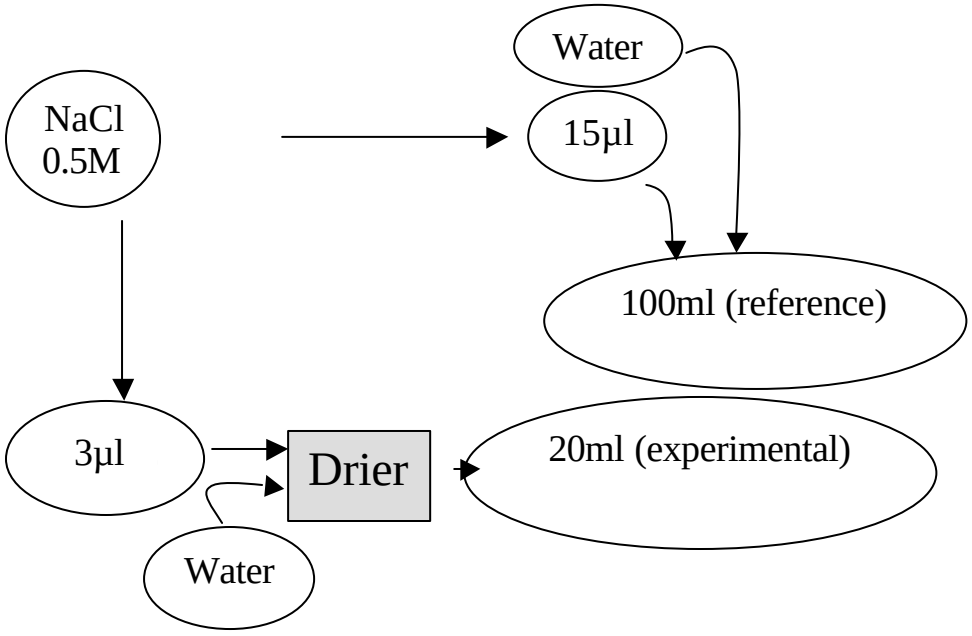

Figure 5-11 schematic view of the experiment to test the recuperation of the solid part in the micro drier

Measurements of conductivity are performed at 24°C. The same test is further performed with a 0.1 M NaCl solution, and the results of all conductivity measurements are summarised in Table 3. From these measurements it is possible to evaluate that the recovery rate of original salt amounts to 94% for the more concentrated solution and to 92% for the less concentrated one.

Original concentration	expected conductivity	experimental conductivity
M	µS	µS
0.5	18.2±0.1	17.1±0.8
0.1	3.6±0.1	3.3±0.3

Table 3 experimental results for measurements of solid part recuperation in the microdrier

5.4 Conclusions

In this chapter two applications based on the structures realised for the flow valves are described. These two applications could find an interesting place in more complex microfluidic systems. The essence of the sample metering system is its capacity to select the exact amount of a liquid sample that is subsequently analysed. This avoids all use of external devices to measure the volume of sample introduced. The advantage following the integration of this element in a chemical analysis cartridge is that such a device does not need to be manipulated by trained personnel.

The second device that is presented allows to change the liquid during a chemical analysis. In the microdrier it is possible to perform the evaporation of a solvent in a closed volume, and recuperate the solid part deposited in

the channel by introducing a new solvent. A further possible use of the microdrier could be the preconcentration of a sample. Integrating the evaporation system with two sample metering systems with different volumes (i.e. 10 µl and 2 µl), it is possible to evaporate the volatile part of the first volume (10 µl) and dissolve the solid part in the second volume (2 µl). in this way the concentration of the sample is enhanced by a factor 5.

6 Cartridge Integration and Characterisation

6.1 Introduction

The sample metering system is integrated in a cartridge (Figure 6-1) formed by a microreactor that can be filled with MIPs, various stop valves gating the flow between the sampling system and the microreactor and between the microreactor and the detection system.

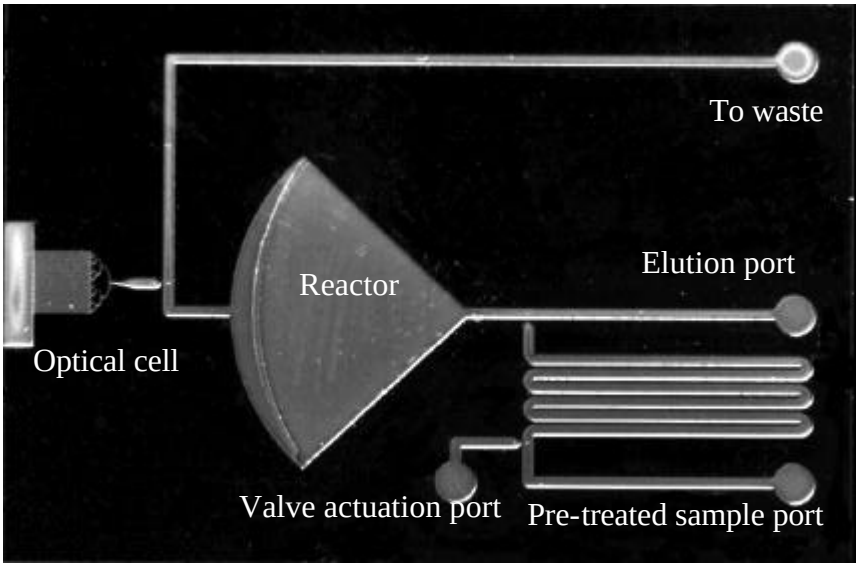

Figure 6-1 picture of the first cartridge design, comprising a7 µl microreactor, a 2 µl metering unit to meter the pre treated sample, and an open tube optical for front end excitation.

The microreactor consists of a flow-through chamber of 7 µl, at the end of which an array of posts is machined to retain the packing material. The geometrical parameters of the microreactor sieve are adjusted taking into account a pattern shrinkage of 3 µm per side caused by the DRIE machining step. The final mesh size results in 22 µm spacing between posts and is

suitable for a use with Ø 25 µm beads. The form of the chamber is adjusted to offer a homogeneous flow resistance in the packed section.

The optical detection cell is placed off-line, i.e. not in the flow through circuit, to allow MIPs packing, sample injection and washing, while ensuring pristine cell conditions. This could prevent clogging by MIP particles not retained by the sieve and contamination by adsorbed species. A stop flow valve similar to those of the sampling unit is used to gate the liquid entry at the optical cell (Figure 6-2). The optical cell design consists of an array of 32 open channels (Figure 6-9). The device is fabricated by DRIE and sealed by anodic bonding with a pyrex cover plate. Channels are 50 µm wide, 2 mm long and 150 µm deep, giving approximately a cell volume of 0.5 µl.

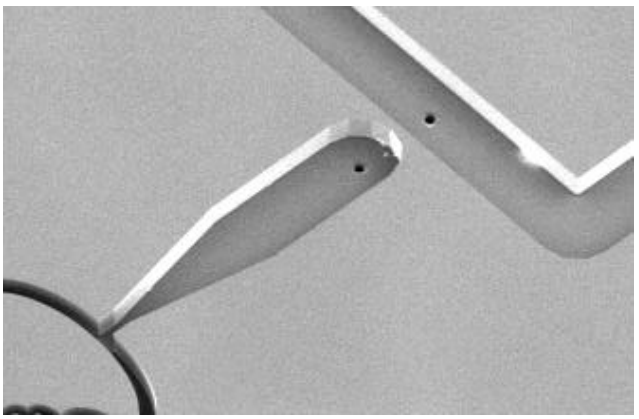

Figure 6-2: stop flow valve separating the optical cell from the fluidic system in the cartridge (SEM image)e

6.2 Microreactor characterisation

Micromachining technology offers unique opportunities for chemical analysis as well as chemical production. The miniaturisation of reactors and

the integration of different components provide new capabilities and functionality, which exceed conventional counterparts.

The functionality advantages of microreactors are small thermal inertia, uniform temperature, short residence time and high surface-volume ratio. Depending on the type of reaction some design considerations are necessary to optimise the microfluidics properties, as fluidic resistance, and functionalities.

For the project CREAM it is necessary to realise a reactor to pack the MIPs for antibiotics recognition. Packing ease and fluidic resistance minimisation are considered the most important features. Different shapes (see Figure 6-3) of microreactors are realised and for each packing tests and fluidic resistance measurements are performed. The shape integrated in the cartridge is the one that assures the bests packing results and the most uniform flow inside the microreactor (Figure 6-5).

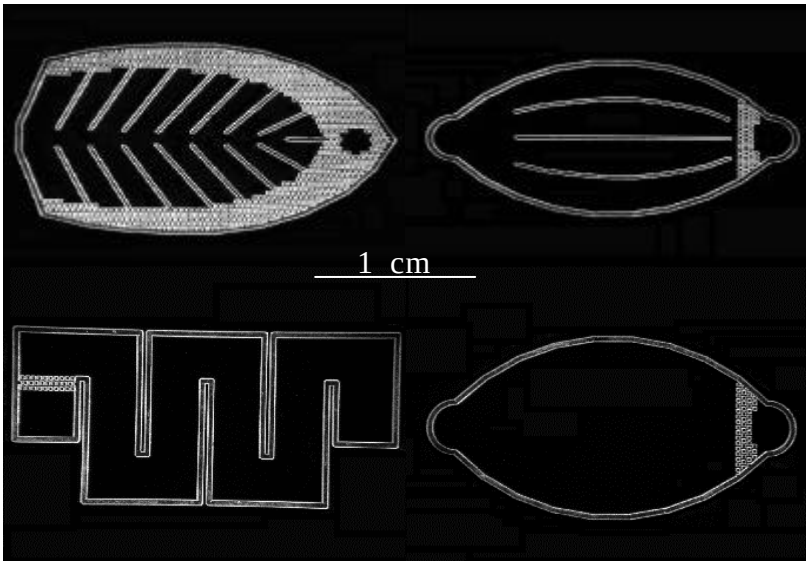

Figure 6-3 different shapes for microreactors

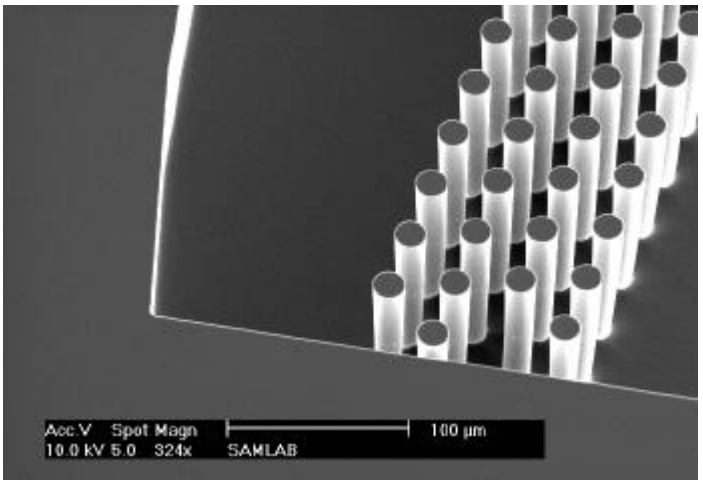

Figure 6-4 view of the in-line sieve – array of posts of Ø 20 µm and 36 µm centre to centre distance (SEM image).

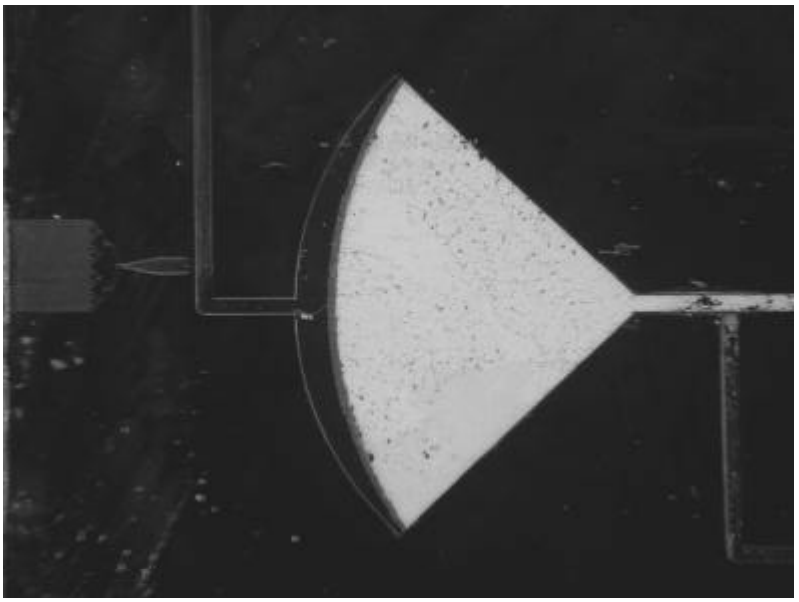

Figure 6-5 picture of the microreactor filled with MIPs

6.2.1 Packing procedure

MIPs are packed using a peristaltic pump; first they are suspended in water (20 ml) with the help of some drop a surfactant (Triton X100), then pumped through the microreactor at 250 µl/min. Once the reactor is almost totally

filled, it is flushed with water under pressure with a water column during about 1 h. If necessary, beads are added and the process repeated. Evaluation of packing quality is performed by observation of the uniformity of the MIPs distribution inside of microreactor.

6.2.2 Fluidic resistance

Assuming that the fluid is Newtonian, the flow regime is laminar, the channel cross-section is rectangular with a channel width w much larger than its height h, the following expression, based on an approximation of the Hagen-Poiseuille equation [53], can be used to evaluate the fluidic resistance in a micro channel:

eq. 19 $$R = \frac{12 h L}{w h^3}$$

where L is channel length and η the viscosity. The resistance R is in $N.s/m^5$. Water viscosity at 20°C is 1.002 centipoises (0.001 Pa.s). The conversion of this resistance in Pa.min/µl, yields:

eq. 20 $$R = 2.004\,10^{-13}\,\frac{L}{w h^3}$$

where L, w and h are in m.

Darcy's law is used in liquid chromatography to relate particle size, liquid flow rate and pressure drop in packed columns or channels:

eq. 21 $$Q = \frac{A k \Delta P}{h L}$$

where Q is the volumetric flow rate, A is the flow area perpendicular to L, κ the permeability of the column, ΔP the pressure drop, η the viscosity and L the column length. The permeability factor can be expressed as:

eq. 22 $$k = \frac{1}{(150 f^2)} \frac{e_o^3}{(1-e_o)^2} \frac{d_p^2}{e_m}$$

Fluidic resistance can simply be defined in both cases as the ratio of pressure drop over flow rate:

eq. 23 $$R = \frac{\Delta P}{Q}$$

The flow rate is estimated by measuring the displacement rate of an air bubble trapped in a graduated tube placed horizontally. Hydrostatic pressure is applied to the system by means of a water column. Results of measurements of volume flow rate as a function of the pressure are shown in Figure 6-6.

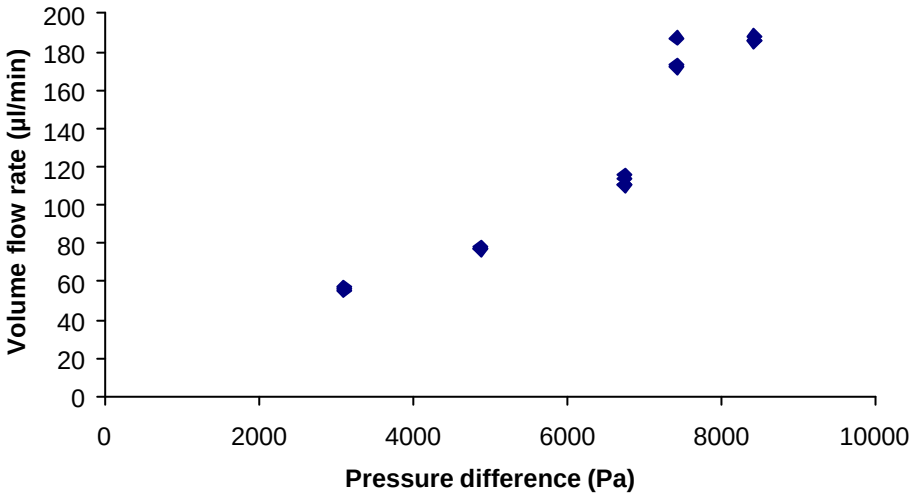

Figure 6-6 characterisation of the fluidic resistance of microreactor integrated in the cartridge, the resistance [Pa min/µl] is given by the reciprocal of the slope of the linear regression

6.3 Optical detection cell characterisation

A new optical detection cell is designed to be integrated in the cartridge. It consists of an array of channels open at the end, the meniscus formed at the

outlet of each channel provided a direct air-liquid interface to the sample volume through which light could be injected (Figure 6-8). With a 90° angle arrangement, i.e. excitation and detection being perpendicular to one another, stray light coupling can additionally be drastically reduced and this further improves the signal quality. To understand the advantages of the adopted design for the optical cell it is compared it with a more traditional design: a simple flow through cell is produced in silicon and Pyrex (Figure 6-7).

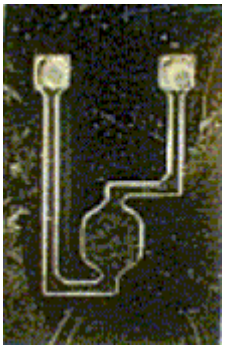

Figure 6-7 flow through optical cell made in silicon and Pyrex.

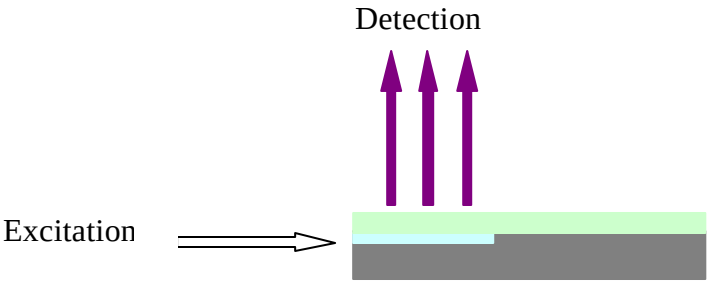

Figure 6-8 schematic of open channel front end excitation cell

6.3.1 Optical detection set-up

The optical bench consists on a deuterium lamp with a constant emission is taken as excitation source, and a photon counting head is integrated in the system to achieve maximum sensitivity. To improve the signal-to-noise ratio the light source and the photodetector are confined into two separate black boxes. Collimating lenses and dichroic mirror are removed and replaced by short segments of optical fibres. This additionally compensates for the low intensity of the lamp and increases the set-up robustness. The power gain by removing these optical elements is estimated to be in the range of 20-30%, distributed to approximately 5% per lens and 10-20 % for the dichroic mirror. Two narrow band pass filters with central wavelength at 334 nm and 394 nm are selected to match the excitation/emission spectra of the selected pyrene derivatives. An optical cell holder is machined to allow accurate and close positioning of the excitation and detection fibres. Filter and lenses assemblies are housed in a robust and light proof aluminium casing with external standard SMA optical fibre connectors to minimise coupling losses and improve optical bench reliability and robustness. The continuous emission expectedly increases the number of photon counts per second, i.e. the signal-to-noise ratio, and extends the dynamic range. Optical cells are characterised by fluorescence with Pyrene butyric acid in acetonitrile (PBAP). In the flow through cell (Figure 6-7) a detection limit in the range of 1 µM is reached with an angle of 54° between the excitation and detection optical fibres. The same calibration experiment with a commercial cuvette lowered the detectable amount to 30 nM. Given an optical path of 100 µm for the optical cell and 1 cm for the commercial device, the results achieved

with the microfabricated device are qualitatively good and are consistent with a one thousand fold reduction of the probed volume.

In the same way the new cell (Figure 6-9) is characterised, in this case the detection is perpendicularly to the plane of the cartridge, and the excitation is in the plane of the cartridge (Figure 6-8). The optical path is increased 20 times compared to the first cell with a fairly similar cell volume.

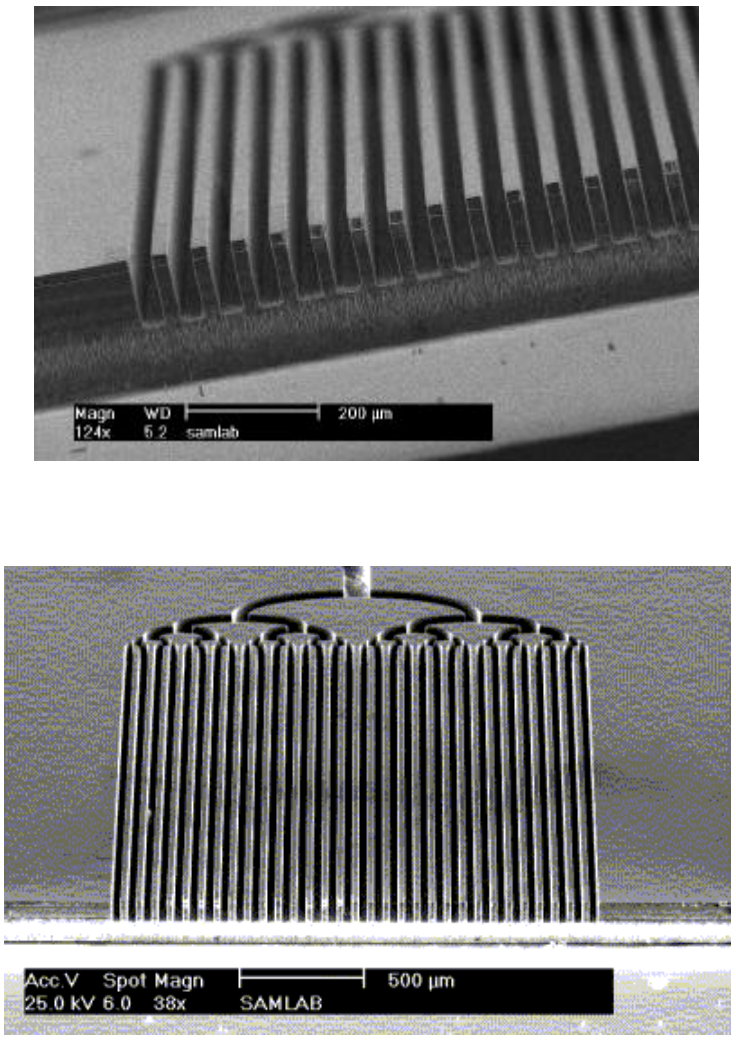

Figure 6-9 SEM images of the open tube optical cell (Pyrex cover plate not shown). The channels are entirely filled by capillarity. The excitation light is injected through the menisci formed at the end of each channel

The detection limit could be lowered to the range of a few 100 nM, directly attributable to a 5 times increase in sensitivity and an improved signal to noise ratio achieved with this 90° excitation/detection configuration (Figure 6-12). The number of background counts could indeed be reduced by a factor of ten. This bench is further used for the detection of PBAP in the final cartridge experiment. The light source is replaced by a more powerful continuous xenon lamp and a new holder for the final cartridge is machined. Preliminary characterisations show that a concentration of 250 nM can be detected with this experimental set-up with a sensitivity of approximately 460 10^9 cps/M. Note that very high noise level this time severely affects the bench performances. This is due to the fact that the cartridge holder is not properly designed. Unfortunately, this could not be corrected on time. It is anticipated that a better signal to noise ratio can be achieved with a proper holder design.

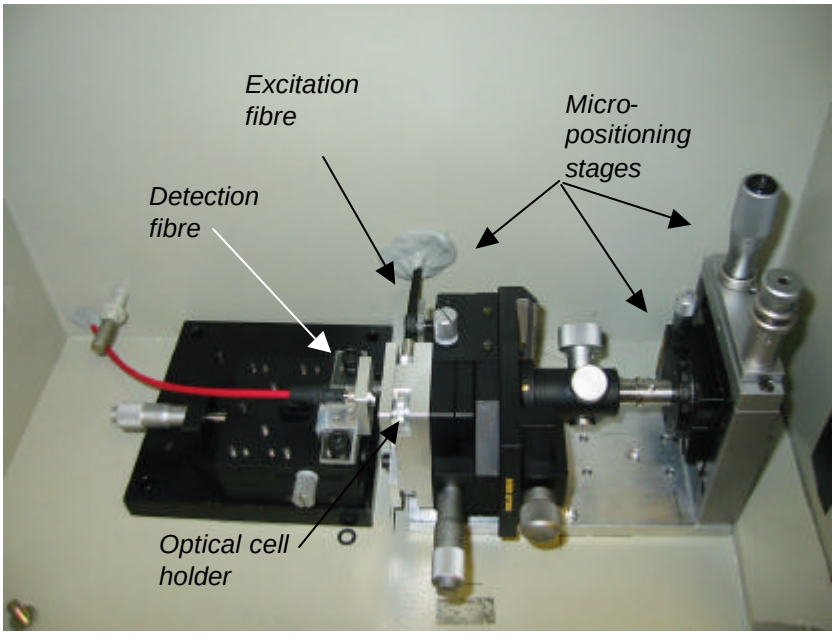

Figure 6-10 picture of the final optical bench design – 90° excitation/detection angle, guided optics

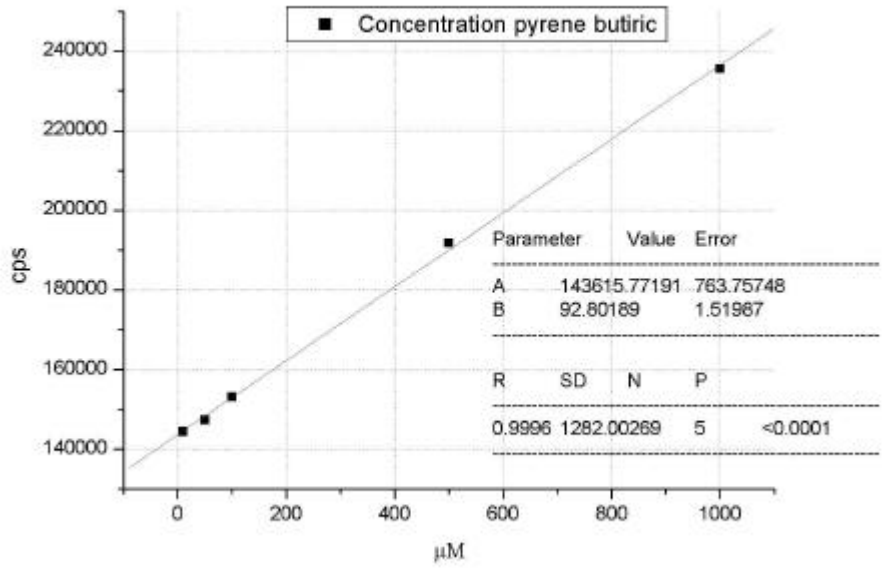

Figure 6-11 calibration curve of Pyrene butyric acid in acetonitrile, achieved with a microfabricated flow through optical cell made of silicon/Pyrex (optical path: 100 µm); linear fit: slope: 90 10^6 cps/M, intercept: 144000 cps (counts per second)

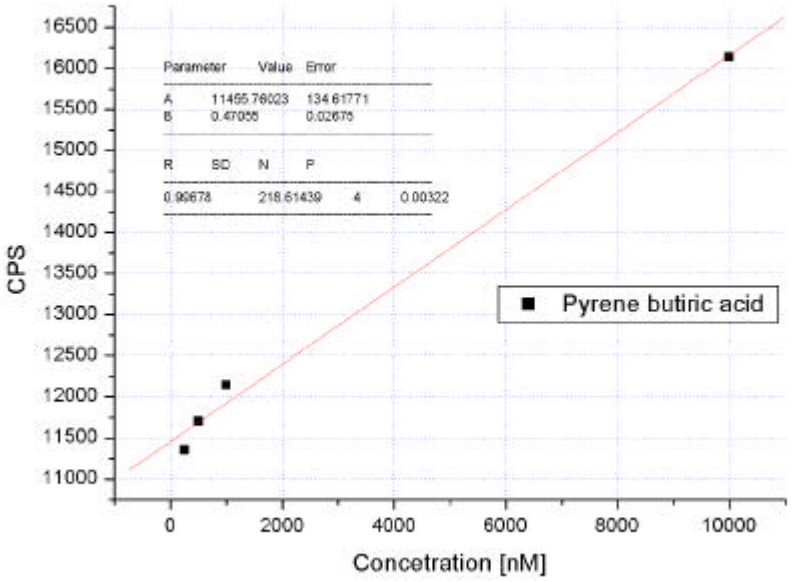

Figure 6-12 calibration curve of Pyrene butyric acid in 99% acetonitrile, achieved with the open tube optical cell (optical path: 2 mm, channel depth 150 µm); linear fit: slope: 470 10^6 cps/M, intercept: 11500 cps (counts per second).

6.4 Conclusions

In this chapter the process for the realisation of the prototype of a microfluidic device is described, in particular it is a cartridge is for the detection of antibiotic residues in milk.

The cartridge is the result of the integration of several microfluidic components that individually best satisfy fluidic requirements, and the whole system is furthermore characterised from fluidic point of view.

The elements that are integrated in the cartridge are the valve and the metering system, described in chapters 4 and 5, the microreactor and the optical detection cell. The developments of these two last components were described in this chapter.

Concerning the microreactor, the attention is focused on its ease of packing the MIPs and on the uniformity of the flux inside the chamber, in order to guarantee the best efficacy possible for the chemical reaction. The new design of the optical cell allows to increase the optical path thus increasing the sensitivity of the optical detection system.

After achieving the realisation of the prototype, the fluidic functionality of the cartridge is verified.

The optical interfaces are developed. The use of guided optics compared to discrete optical lenses improve the robustness and detection performances. The use of a continuous light source with the photon counting unit offers the best sensitivity, compared to a pulsed lamp. With this configuration a concentration of 250 nM PAAP could be detected in the cartridge optical cell.

7 Conclusions

Microfabrication technology has proven to be a valuable tool for creating miniaturized devices for applications in chemical and biochemical assays. The attractive features associated with these devices include their potential for system integration (in which various assays are included onto the fluidic platform), speed, reduced sample and reagent consumption, high efficiency and automation. Moreover, microdevices are small, compact and easy to transport. They therefore represent a good route to achieve real-time analysis.

All along this work different fabrication technologies and microfluidic elements have been developed. By the integration of these microfluidic elements it is possible to realize devices for specific applications (measurement of ammonia and monitoring of antibiotic residues in milk). Interesting results are achieved with the development of the plastic replication technique, that allows an extremely large flexibility concerning the devices' shape, and a low cost.

A further result is the realisation of the passive stop flow valve that shows to have interesting potential applications. These elements are able to gate between two different components of a microfluidic system, and they can find place in more complicated unit with specific functionalities. Two microfluidic devices are been developed using the stop flow valve: a sample metering system and a microdrier.

The sample metering system is used to dose in a precise way a chemical compound, such a device, integrated in a cartridge, allow to perform chemical analysis in site without the help of specific dosing tools.

The microdrier allow to change the liquid during a chemical analysis, performing the evaporation of a solvent, and recovering the solid part deposited by introducing a new solvent.

Finally some microfluidic elements are integrated in a new cartridge. A microreactor, that can be packed with MIPs, is characterised from the fluidic point of view. The microreactor is integrated with a sample metering system and an optical detection cell, finally the whole system is characterised in its microfluidic properties. This cartridge is developed for the project CREAM and constitutes the first prototype.

8 References

[1] “High quality imaging system for color inkjet printers using a piezoelectric print head”, K. Shimada, Proceedings. IS&T's PICS Conference. 51st Annual Conference. Soc. Imaging Sci. & Technol. 1998, pp.424-6.

[2] “Hydrodynamic model for particle clustering in electrophoretic deposition.” J. Feng, Y. Xu SPIE-Int. Soc. Opt. Eng. Proceedings of Spie - the International Society for Optical Engineering, vol.3877, 1999, pp.130-8.

[3] “Microfabricated separator and manipulator of blood cells for health care devices” T. Ujiie, A. Yamazaki., M. Watanabe, T. Okuda, T. Ichiki, Y. Horiike, Digest of Papers Microprocesses and Nanotechnology 2000. 2000 International Microprocesses and Nanotechnology Conference (IEEE Cat. No.00EX387). Japan Soc. Appl. Phys. 2000, pp.28-9.

[4] “Fabrication of a microfluidic cell analyzer in a microchannel using impedance spectroscopy”, S. Gawad, M. Henschkel, Y. Leung-Ki, R. Iuzzolino, L. Schild, P. Lerch, P. Renaud,1st Annual International IEEE-EMBS Special Topic Conference on Microtechnologies in Medicine and Biology. Proceedings (Cat. No.00EX451). IEEE. 2000, pp.297-301.

[5] “Development of biofactory-on-a-chip technology”, Z. Xiao-Feng, J.P. Burt, M.S. Talary, A.D. Goater, R. Pethig, SPIE-Int. Soc. Opt. Eng. Proceedings of Spie - the International Society for Optical Engineering, vol.4177, 2000, pp.241-50.

[6] “In situ fabricated porous filter - characterization and biological applications” J. Moorthy, D.J. Beebe, 2nd Annual International IEEE-

EMBS Special Topic Conference on Microtechnologies in Medicine and Biology. Proceedings (Cat. No.02EX578). IEEE. 2002, pp.514-17.

[7] “Hybrid macro-micro fluidics system for a chip-based biosensor” C.R. Tamanaha, L.J. Whitman, R.J. Colton, Journal of Micromechanics & Microengineering, vol.12, no.2, March 2002, pp.N7-N17.

[8] “Scheduling of microfluidic operations for reconfigurable two-dimensional electrowetting arrays” J. Ding, K. Chakrabarty, R.B. Fair, IEEE Transactions on Computer-Aided Design of Integrated Circuits & Systems, vol.20, no.12, Dec. 2001, pp.1463-8.

[9] “The impact of MEMS on the chemical and pharmaceutical industries”, K.F. Jensen Technical Digest. Solid-State Sensor and Actuator Workshop (TRF Cat. No.00TRF-0001). Transducers Res. Found. 2000, pp.105-10.

[10] “Implications of microreactors for chemical synthesis”, S. Taghavi-Moghadam, A. Kleemann, S. Oberbeck, Proceedings. MICRO.tec 2000. VDE World Microtechnologies Congress. VDE Verlag. Part vol.2, 2000, pp.489-91 vol.2.

[11] “Optimal design for flow uniformity in microchannel reactors”, J.M. Commenge, L. Falk, J.P. Corriou, R. Matlosz, Proceedings. MICRO.tec 2000. VDE World Microtechnologies Congress. VDE Verlag. Part vol.1, 2000, pp.375-9 vol.1.

[12] “Technologies and devices for micro chemical systems”, H. Gardeniers, R. Schasfoort, A. van den Berg, Mst News, no.4, Sept. 2000, pp.10-12.

[13] “Ultrasonic micromixer for microfluidic systems”, Z. Yang, H. Goto, M. Matsumoto, R. Maeda, Proceedings IEEE Thirteenth Annual International Conference on Micro Electro Mechanical Systems (Cat. No.00CH36308). IEEE. 2000, pp.80-5.

[14] “Development of integrated microfluidic system for genetic analysis”, R.H. Liu, P. Grodzinski, Journal of Microlithography, Microfabrication, & Microsystems, vol.2, no.4, Oct. 2003, pp.340-55.

[15] “Microfluidic chips for DNA amplification, electrophoresis separation and on-line optical detection”, Gwo-Bin Lee, Che-Hsin Lin, Fu-Chun Huang, Chia-Sheng Liao, Chia-Yen Lee, Shu-Hui Chen, Proceedings IEEE Sixteenth Annual International Conference on Micro Electro Mechanical Systems (Cat. No.03CH37426). IEEE. 2003, pp.423-6.

[16] “A novel strategy for the design of multiple reaction systems for genetic analysis” M. Krishnan, S.N. Brahmasandra, D.T. Burke, C.H. Mastrangelo, M.A. Burns, Elsevier. Sensors & Actuators A-Physical, vol.A95, no.2-3, 1 Jan. 2002, pp.250-8.

[17] “Generation of concentration gradient by controlled flow distribution and diffusive mixing in a microfluidic chip”, Y. Mengsu, Y. Jun, L. Cheuk-Wing, Z. Jianlong Lab on a Chip, vol.2, no.3, Aug. 2002, pp.158-63.

[18] “High-density plastic microfluidic platforms for capillary electrophoresis separation and high-throughput screening” A. Gerlach, G. Knebel, A.E. Guber, M. Heckele, D. Herrmann, A. Muslija, T. Schaller, Sensors & Materials, vol.14, no.3, 2002, pp.119-28.

[19] “Biology lab-on-a-chip for drug screening” H. Salimi-Moosavi, R. Szarka, P. Andersson, R. Smith, D.J. Harrison Technical Digest. Solid-State Sensor and Actuator Workshop. Transducer Res. Found. 1998, pp.350-3.

[20] “Miniaturized Integrated Analytical Test Container”, C.M. Coleman, US patent N° 3,799,742

[21] “Automated Chemical Analyzer”, W.E. Blackburn, US patent N°3,497,320

[22] “Miniaturized Total Chemical Analysis Systems – A Novel Concept for Chemical Sensing”, A. Manz, N. Graber, H.M. Widmer, Sensors & Actuators B, 1 (1990) 244

[23] “Micro Total Analysis Systems. 1. Introduction, Theory, and Technology”, D.R. Reyes, D. Iossifidis, P.-A. Auroux, A. Manz, Anal. Chem. 74 (2002) 2623

[24] “Micro Total Analysis Systems. 2. Analytical Standard Operations and Applications”, P.-A Auroux, D. Iossifidis, D.R. Reyes, A. Manz, Anal. Chem. 74 (2002) 2637

[25] “Microfluidics - a review”, P. Gravesen, J. Branebjerg, O.S. Jensen, J. Micromech. Microeng, 3 (1993) 168

[26] ”Towards integrated microliquid handling systems “ M. Elwenspoek, T.S.J. Lammerink, R. Miyake, J.H.J Fluitman, J. Micromech. Microeng., 4 (1994) 227

[27] “Fundamentals of Microfabrication”, M. Madou, CRC press, 1997, New-York, USA

[28] “Deep reactive ion etching: a promising technology for micro- and nanosatellites” Ayon AA, Bayt RL, Breuer KS, Smart Materials & Structures, vol.10, no.6, Dec. 2001, pp.1135-44.

[29] “Polymer Microfabrication Methods for Microfluidic Analytical Applications”, H. Becker, C. Gärtner, Electrophoresis, 21 (2000) 12

[30] “Comparison of two passive valve designs for microlamination architecture”, B. K. Paul, T. Terhaar, Journal of Micromechanics & Microengineering, vol. 10, n. 1 (2000) pp. 15-20.

[31] “Miniature on-shot valve”, L.J. Guerin, O. Dubochet, J-F. Zeberli, P. Clot, P. Renaud, Proceedings MEMS 98, pp. 425-428

[32] “An analytical model for passive microvalves”, M. Carmona, S. Marco,J. Samitier, M.C. Acero, J.A. Plaza, J. Esteve, Sensor & Materials, vol. 13, n. 7 (2001) pp.373-383

[33] “ High-Pressure Microfluidic Control in Lab-on-a-Chip Devices Using Mobile Polymers Monolyts”, E. F. Hasselblink, T. J. Shepodd, J. E. Rehm, Analytical Chemistry, vol 74 (2002) pp. 4913-4918.

[34] “Nanoliter Liquid Metering in Microchannels Using Hydrophobic Patterns”, K. Handique, D.T. Burke, C. H. Mastrangelo, M. A. Burns, Analytical Chemistry, 72, 4100 (2000) and world patent WO 02/07884

[35] “Hydrophobic Microfluidics”, M.R. McNeely, M.K. Spute, N.A. Tusneem and A.R. Oliphant, proc. SPIE conf. on Microfluidic Devices and Systems II, vol 3877, p. 210 (1999)

[36] “Fabrication and Characterization of Three-Dimensional Microfluidic Arrays”, S.M. Kugelmass, C. Lin, S.H. DeWitt, Proc SPIE conf on Microfluidic Devices and Systems II, 3877, 88 (1999) [US patent N° 6,117,396]

[37] "Microfabricated Capillarity-Driven Stop Valve and Sample Injector,", P.F. Man, C. H. Mastrangelo, M. A. Burns, and D. T. Burke, MEMS Conference Proceedings (1998) 45

[38] “New materials for electrochemical sensing IV. Molecular imprinted polymers”, A. Mercoçi and S Alegret, Trends in analytical chemistry, vol. 21 No.11, p. 717 (2002)

[39] “Molecular imprinting: at the edge of the third millennium”, S.A. Piletsky, S. Alkok and A.P.F. Turner, Trends in Biotechnology, vol. 19, No. 1, p. 9 (2001)

[40] “Molecular imprinted polymers: useful materials for analytical chemistry?” A.G. Mayes and K. Mosbach, Trends in analytical chemistry, vol. 16 No.6, p. 321 (1997)

[41] “Molecular imprinted polymers and their use in biomimetic sensor”, K. Haupt and K. Mosbach, Chem. Rev., Vol.100 p 2945 (2000)

[42] “Moleculary imprinted polymers and optical sensing application”, S. Al-Kindy, R. Badia, J.L. Suárez-Rodríguez and M.E. Díaz-García, Critical reviews in Analytical Chemistry, Vol. 30, no. 4, p 291 (2000)

[43] “Molecularly imprinted polymers. Manmade mimics of antibodies and their applications in analytical chemistry”, B. Sellergren, Elsevier, Amsterdam, 2001

[44] “Ammonia detection by use of near-infrared diode-laser-based overtone spectroscopy”, Claps R, Englich FV, Leleux DP, Richter D, Tittel FK, Curl RF, Applied Optics, vol.40, no.24, 20 Aug. 2001, pp.4387-94.

[45] “Amperometric ammonia sensor using polypyrrole and substituted polypyrrole with different dopants”, Dall'Antonia LH, Miyata MEV, de Torresi SIC, Chemical and Biological Sensors and Analytical Methods II Proceedings of the International Sympsoium (Electrochemical Society Proceedings Vol.2001-18). Electrochemical Society. 2001, pp.76-81.

[46] “Fluorometric determination of ammonia in sea and estuarine waters by direct segmented flow analysis”, Kérouel R, Aminot A, Marine Chemistry, vol. 57 (1997), pp. 265-275.

[47] “Ammonia detection using nanoporous alumina resistive and surface acoustic wave sensors”, Varghese O K, Gong D, Dreschel W R, Ong K G and Grimes C A, Sensor and actuators B, vol. 94 (2003), pp 27-35.

[48] “A simple and precise method for measuring ammonium in marine and freshwater ecosystems”, Holmes R M, Aminot A, Kérouel R, Hooker B A,

Peterson B J, Canadian Journal of Fisheries and Aquatic Science, vol. 56 (1999), pp. 1801-1808.

[49] “The Machanism of Field-assisted Silicon-glass Bonding”, Y. Kanda, K. Matzuda, C. Murayama and J. Sugaya, Sensors and Actuators, A21-A23 (1990) , 939-943

[50] “Miniaturized genetic analysis system”, R. C. Anderson, G. J. Lipshutz, International Workshop on Solid-State Sensor and Actuators (Hilton Head ’96) pp. 258-261, 1996.

[51] “Physical Chemistry”, W.J Moore, Prentice-Hall, Englewood Cliffs, 1972.

[52] “Fundamental and applications of Microfluidics”, N-T Nguyen, S. T. Wereley, Artech House Inc., Boston.

[53] “Fluid Mechanics”, F. M. White, McGraw-Hill series in mechanical engineering, 4th ed., Boston, 1999

9 Acknowledgements

My swiss odyssey started during my fellowship in bioelectronics: in July 2000 I went to Basel for a congress (IMCS) and I found a brochure about the Institute of Microtechnology of Neuchâtel. Being come back to Italy, my attention was caught by the Sensors, Actuators and Microsystems Laboratory for the interest of activity developped. Armed of enthusiasm and thirst of new interesting experiences, I wrote an e-mail to Prof. Nico de Rooij asking him if there was a chance to continue my fellowship in his lab. Having specified that I had my Italian fellowship and it wasn't necessary to support me in any financial aspect from him…the answer arrived two hours later: "Ok, you will be welcome, when could you come? Next week?" So, the 25th of august I meet Dr. Eva L'Hostis in Neuchâtel in order to see which possibilities the project offered me and in which part I was going to be integrated. Oh My God! With my poor French and few words in English I could use, this meeting had been a little bit startling! My strongest full immersion course of French was already started!

For these reasons the first thanks go to Nico for having given me this opportunity.

After the meeting in August, I moved up from Italy to Neuchâtel the 25th of September to start my stage, and in the same day I met Dr. Jean Charles Fiaccabrino, the CREAM project leader, that I thank for having agreed to integrate my as a member of his staff.

Thanks to you, Eva, my mentor in the clean room and in the chemical lab, you succeed in teaching me a lot of things about microfabrication…but I am

still sorry for not being your ideal student for chemistry, but I hope that I gave you a lot of satisfaction as a French student!

After these first ten months of training, my stay had been converted as doctoral study in the same team.

I especially would like to tank my colleagues Quyên and Vincent who have became also good friends: we shared a lot of good moments in the lab and outside (I think Edit and Gianni will remember us for a long time about our “performances” in the white room).

I thank all the colleagues that make pleasant my stay at IMT, with their humour, conviviality and fun, always ready for amusing initiatives in the dinning breaks and sketches, thanks Laure, Seb, Gianluca, Alexandra, Olivier, Kaspar…

Many tanks to Peter, who gave me advices and support in the chemical lab after the leaving of Eva. Also to have helped me with my thesis redaction. Thanks to Milena to accept to be an expert for my exams and for all other professional and human advices.

I would like to mention the technical staff, Edit and Gianni, who have been able to resolve all little and big troubles in technologic process and for having been a good public for our folly (see before about Quyên and Vincent), Sylvain, Pierre-André (Clairon), Nicole, José et Sabina for their help and patience in the clean room and Sylviane in the chemical lab.

Again I would like to mention my room mate who accompanied all my stay, Andreas and Teru (I am sorry for you, Teru, that you still have to bear the german calls of Andreas!).

Tanks to Mireille and Massoud for their joviality and sarcasm.

Tanks to Florence for the secretarial help and for having administrated my (psyco-)medicines when, in the morning, I had forgotten them.

Again Laura, Yves, Luca, Giovanni, Danik, Maurizio, Raphäel, Sander, Winston and all the other colleagues, with whom, for different reasons, I had productive interactions.